



Grant agreement no. 243964

QWeCI

Quantifying Weather and Climate Impacts on Health in Developing Countries

D2.1a Report on dynamic malaria model runs for regions of interest and verification against datasets

Start date of project: 1st February 2010

Duration: 42 months

Lead contractor: UNILIV
Coordinator of deliverable: UNILIV
Evolution of deliverable

Due date : M15
Date of first draft : M17
Start of review : M18
Deliverable accepted : M18

Project co-funded by the European Commission within the Seventh Framework Programme (2007-2013)		
Dissemination Level		
PU	Public	PU
PP	Restricted to other programme participants (including the Commission Services)	
RE	Restricted to a group specified by the consortium (including the Commission Services)	
CO	Confidential, only for members of the consortium (including the Commission Services)	

D2.1a Report on dynamic malaria model runs for regions of interest and verification against datasets	1
1- Preamble	3
2- Method.....	3
The Liverpool Malaria model	3
Climate datasets and LMM runs	4
Diagnostics.....	5
3- Results	5
Senegal	5
Ghana	6
Malawi	7
South Africa.....	8
4- Summary table and perspectives	9
References.....	10
Figures.....	11

1- Preamble

Malaria results in over one million deaths annually, with over 80% of these fatalities occurring in sub-Saharan Africa (WHO, 2005). Malaria is caused in humans by infection with the protozoan *Plasmodium*, and is transmitted between humans by female mosquito vectors from the *Anopheles spp.* The first symptoms are relatively similar to those of seasonal flu, with fever, sore throat, pain, chills and aches; and sometimes nausea and diarrhoea that can lead to more serious health issues. Infection with the most severe form of the parasite, *Plasmodium falciparum*, if not promptly treated, may lead to kidney failure, seizures, mental confusion, coma, and death. Epidemics of the disease can be triggered by factors affecting human, vector or parasite populations including abnormal meteorological conditions, changes in anti-malarial programs, population movement, and environmental changes (Nájera et al., 1998). The mosquitoes' breeding sites (ponds) and the lifecycle of the malaria parasite are both strongly connected to climatic variability, especially rainfall and temperature. Climate-driven models of malaria provide a quantitative method of considering the impact of one of these factors.

In this document, we aim to model the malaria patterns based on climatic drivers for targeted African countries (Senegal, Ghana, Malawi and South Africa). The Liverpool Malaria Model (Hoshen and Morse, 2004) is utilised to model the malaria patterns and different climate datasets are employed to achieve such a task. The malaria simulations are then compared and validated against observed datasets (when available) and existing risk maps created by former international research projects.

2- Method

The Liverpool Malaria model

The Liverpool Malaria Model (LMM 2004) (Hoshen and Morse, 2004) uses a dynamic approach to simulate malaria incidence in the human population, and consists of two climate driven components. Firstly, the mosquito population is modelled using larval and adult stages, with the number of eggs deposited into breeding sites depending on the previous ten days' (dekadal) rainfall, the larval mortality rate also dependent on dekad rainfall, an adult mosquito mortality rate dependent on temperature, and the egg-laying/biting (gonotrophic) cycle also dependent on temperature. Secondly, the process of parasite transmission between human and mosquito hosts is modelled simulated, with temperature-dependencies in the rate of development of the parasite within the mosquito (sporogonic cycle) and the mosquito biting rate. Both the sporogonic and gonotrophic cycles progress at a rate dependent on the number of "degree days" above a specific temperature threshold. The gonotrophic cycle takes approximately 37 degree days with a threshold of 9°C, whereas the sporogonic cycle takes approximately 111 degree days with a threshold of 18°C. This latter threshold is one of the most critical areas of sensitivity in the model, and below it no parasite development can occur. Further details of the model are given elsewhere (Hoshen and Morse, 2004; Morse et al., 2005). An updated version of the model (LMM 2010) using another set of parameters and different egg, larval and mosquito survival schemes has been carried out by Ermert et al., 2011a and 2011b. Ermert et al. showed improvements in simulating malaria dynamics over sub-Saharan Africa using this model version. However, in this document we only employ the original version of the LMM (an extended comparison between both model versions will be performed later on within WP2.1).

Climate datasets and LMM runs

In order to model and to map malaria, several climatic observation datasets are utilised. As a reminder, the LMM uses daily rainfall and daily temperature as inputs.

Various sets of gridded daily rainfall products have been employed:

- Mixed satellite and rain gauges observations from the Global Precipitation Climatology Project (GPCP) dataset (Huffman et al, 2001).
- Mixed satellite and rain gauges observations from the NASA Goddard Space Flight Center Tropical Rainfall measuring mission (TRMM) dataset (Huffman et al, 2001).
- Rainfall products based on NCEP-NCAR (Kalnay et al, 1996) and ERAINTERIM (Uppala et al, 2008) reanalysis (blend of climate model outputs and various sources of observations using complex assimilation methods).

Daily temperatures are estimated using NCEP-NCAR (Kalnay et al, 1996) and ERAINTERIM (Uppala et al, 2008) reanalysis. Different LMM model runs have been carried out. A one year spin-up is first performed, based on the mean daily rainfall and temperature cycle. The model has been run using ERAINTERIM and NCEP rainfall and temperature, and two hybrid runs using GPCP/TRMM satellite rainfall estimates and ERAINTERIM temperatures have also been produced (in this case the temperature data has been interpolated on the rainfall data grid). Table 1 summarizes the different model runs (time periods, spatial resolution, etc.).

Malaria Simulation	Period	Spatial Resolution	Comments
NCEP	1980-2010	2°x2° (~200km ²)	Coarse datasets. Large rainfall biases over West Africa.
ERAINTERIM	1989-2010	1°x1° (~100km ²)	Better reanalysis product than NCEP and former ERA40 reanalysis products for West Africa.
GPCP-ERA	1997-2007	1°x1° (~100km ²)	Rainfall from GPCP satellite estimates and temperature from ERAINTERIM reanalysis.
TRMM-ERA	1998-2010	0.25°x0.25° (~25km ²)	Rainfall from TRMM satellite estimates and temperature from ERAINTERIM reanalysis. Most relevant dataset to use at the country level for impact applications (higher resolution).

Table 1: Summary of input data for malaria simulations performed with the LMM.

The Climatic Research unit (CRUTS2.1) dataset at 50km² resolution is also employed to validate the mean climatic features for the targeted countries (Mitchell et al., 2004) for the period 1950-2002. This dataset is based on station measurements. As only monthly means were available, no LMM simulations were performed based on this dataset.

Diagnosics

For each country namely for Senegal, Ghana, Malawi and South Africa:

- Mean seasonal cycle maps and indices (from January to December) are given for rainfall, temperature, malaria incidence and prevalence (proportion of population infected).
- The mean annual simulated malaria prevalence patterns based on the different runs are inter-compared and validated against other published materials (MARA-ARMA project).
- Annual rainfall, temperature and malaria prevalence anomalies are then discussed for the recent period: 2000-2010 (as most of the collected malaria data are not available before 2000).

3- Results

Senegal

Senegal is located in Western Africa, and borders the North Atlantic Ocean, between Guinea-Bissau and Mauritania. At latitudes of 3 to 12°N, most of Senegal has a typically tropical climate, but the northern regions lie in the sub-tropical semi-arid belt called the Sahel. The topography of Senegal consists mainly of rolling sandy plains, but rises to hills in the south-east. The rainy season is dominated by the south-east monsoon winds, and a dry season dominated by the dry Harmattan coming from the north-east. Most of the rains occur between May and November, with large amounts of precipitation occurring from June to the end of September, with a rainfall peak in August (Fig S1-S3). There is a clear meridional gradient of precipitation with the largest rainfall occurring south of 14°N, and the driest area bordering Mauritania. The onset of the rainy season takes place in late May/early June over the southern part of the country, with the latest rains occurring during the first decade of August in the northern part. The rainfall pattern mainly follows the northward course of the inter-tropical convergence zone (ITCZ). Generally, temperatures in Senegal increase from the coast towards the east of Senegal in most seasons. The warmest temperatures occur over the eastern part of the country from April to June (35°C), whilst the cooler coastal regions are 25 to 28°C (Fig S1-S2). In the cooler seasons (Oct-Nov-Dec and Jan-Feb-Mar), average temperatures can be below 25°C at the coast and up to 30°C in the west (Fig S2). A severe drought affected the country from in the early 1980s with significant social and economic impacts, whilst high rainfall occurred in the early 1960s. The temperatures have increased by about 0.9°C since the 1960s over Senegal.

The simulated malaria incidence belt reaches its furthest northward location (14-15°N) in the boreal autumn (Sept-Oct-Nov, see Fig S4). There is a lagged relationship between rainfall and malaria incidence seasonality (Fig S1). High malaria incidences are conditioned by the climatic conditions occurring two months before. Indeed the peak in rainfall occurs in August while the peak in malaria incidence is simulated in October. High malaria prevalence is simulated from October to January. These findings are consistent with the results raised by field observations (number of observed malaria cases over the Linguere and Dahra district of northern Senegal, not shown). However, the LMM underestimates the top northward location of the malaria incidence belt compared to other modelling approaches, which show the northern epidemic fringe of malaria incidence extending to 17°N (Le Sueur et al, 1997). As a consequence, the simulated seasonality of malaria over Senegal is well represented, but the interannual variability is underestimated with respect to malaria cases observation in the northern part of Senegal (similar results have been shown for northern Niger by Caminade et al., 2011).

The simulated annual mean prevalence of malaria for different driving observed datasets is shown in FigS5a. The coarse spatial resolution of the NCEP and ERAINTERIM runs provides limited information at the country level. The TRMM-ERA1 and GPCP-ERA1 highlight similar features,

with the highest prevalence being simulated over the southern part of the country, and the lowest one in the northern part. The malaria epidemic fringe (depicted as high COV namely dark blue areas on FigS5b) is located around 15°N for the TRMM-ERA-Interim LMM simulation. The distribution of endemic malaria based on the MARA-ARMA model (Fig S5c) shows that most of Senegal is considered as endemic, while the malaria fringe is shown to be located further north (around 17°N, at the border of Senegal and Mauritania).

The annual anomalies of rainfall, temperature and malaria prevalence are respectively shown on Fig FigS6a, FigS6b and Fig S6c. The simulated lower than average malaria years (2002, 2006, and 2007) are generally related to drier conditions. The temperature anomalies for these years are respectively warmer, slightly cooler and cooler than average. The “high” malaria years (2009, 2010) are linked to wetter than average conditions; the highest year (2010) being associated with large precipitation and warmer than average conditions.

Ghana

Ghana is located in West Africa, on the Gulf of Guinea coast. The climate of Ghana is typically tropical and is strongly dominated by the West Africa monsoon. The rainfall seasons over Ghana are conditioned by the movement of the tropical rain belt (or ITCZ). The first large rainfall peak occurs in May-June when the rain belt is moving northward, followed by a short dry season in July-August (more marked in the south); and the second peak is observed in September-October during the southward retreat of the ITCZ (Fig G1-G2). Northern Ghana experiences a shorter rainy season (June-September) when the rain belt is at its northern position, while southern Ghana (tropical) experiences more precipitation all year long. Seasonal variations in temperature in Ghana are greatest in the north, with highest temperatures in the hot, dry season (from March to June) at 27-30 °C and lowest in Jul-Aug-Sept at 25-27°C (Fig G1-G3). Further south, temperatures reach 25-27°C in the warmest season Feb-Mar, and 22-25°C at their lowest in Jul-Aug-Sept, during the establishment of the West African monsoon. Mean annual temperatures have increased by about 1.0°C over Ghana since the 1960s at an average rate of .021°C per decade. Like other West African countries, rainfall was particularly high during the 1960s whereas a significant drought was observed during the 1970s and the early 1980s.

Like in Senegal, there is a lagged relationship between rainfall and malaria incidence seasonality over Ghana (Fig G1). High malaria incidences are also conditioned by the climatic conditions occurring two months before. High malaria incidences are simulated from June to February. The largest malaria incidence (above 60%) is simulated in Aug-Sept-Oct-Nov. High malaria prevalence is simulated from August to January (Fig G1). Generally, malaria incidence is only low over Ghana from February to April (Fig G4). Large malaria incidence is simulated from August to November over the northern half of the country, while high malaria incidence is shown almost all year round over southern Ghana (from May to January). Low malaria incidence is also depicted over the grid points bordering the southern coasts of Ghana. As denoted by experts in Ghana (KNUST), the months from December to February indeed record low malaria incidence in the forest belt in particular within the vicinity of Kumasi. The malaria seasonal plots seem very representative; in particular they represent the actual seasons of malaria incidence and endemic zone. However, the low mean malaria incidence around the Volta Basin and the entire south Eastern part of Ghana appear to be underestimated by the model. Also 20 – 40 % malaria incidence in the southern part of the country, in particular around Aflao, Denu, Keta, Ada, Accra-Tema, Cape Coast and Sekondi-Takoradi for the months of June through to November may not be correct as these parts of the country are densely populated; and as a result, a number of natural lagoons which serve as additional mosquito breeding sites are present in these areas. This means that a high malaria incidence is expected in those months in southern Ghana.

The simulated annual mean prevalence of malaria for different driving observed datasets is shown on FigG5a. The coarse spatial resolution of the NCEP and ERAINTERIM runs still provides limited information at the country level. However, the southern half of the country exhibits high prevalence, indicating that malaria is highly endemic. The TRMM-ERA1 and GPCP-ERA1 highlight similar features, with the highest prevalence being simulated over the southern part of the country. There are still moderate/high values of malaria incidence in the North, and a local minimum is simulated near the coasts bordering the Gulf of Guinea. The magnitude of prevalence is significantly higher than the one simulated over Senegal (note that the simulated prevalence by this version of the LMM cannot extend 65%). The malaria COV (FigG5b) over Ghana is relatively low, except over the southern coasts for the high resolution simulations (TRMM-ERA1). This means that the interannual variation of the malaria incidence is relatively small with respect to the long-term average over Ghana (denoting an “endemic or seasonal endemic” profile). If we define the epidemic fringe by a COV above 0.5, only the southern coasts fit this profile. These results are relatively consistent with those raised during the MARA-ARMA project (Fig G5c), which shows that malaria is endemic over the whole country excepting over small patchy areas located on the southern coasts. The annual anomalies of rainfall, temperature and malaria prevalence are respectively shown on FigG6a, FigG6b and Fig G6c. The lowest simulated malaria year (2001) is associated with drier and slightly cooler climatic conditions. In 2007, malaria is simulated to be low over the western part of the country where warmer and drier conditions occurred. The high malaria years (2009, 2010) are concomitant with wetter and warmer than average climatic conditions.

Malawi

Malawi is located in eastern southern Africa and extends across the latitudes 9-15°S. The country’s topography is highly varied; the Great Rift Valley runs north to south through the country, containing Lake Malawi, and the landscape around the valley consists of large plateau at an elevation of around 800-1200m, but with peaks as high as 3000m. The country’s climate is tropical, but the influence of its high elevation means that temperatures are relatively cool with respect to the western African countries. The rainfall seasons over Malawi are conditioned by the movement of the ITCZ. The first significant rain occur in November, and the rainy season extends until the following April (Fig M1). In the south of Malawi the wet season normally lasts from November to February, but rain continues into March and April in the north of the country as the ITCZ migrates northwards (with the highest rain occurring in Jan-Feb-Mar, Fig M1-M2). Topographical influence also causes local variations to the rainfall with the highest altitude regions receiving the highest rainfalls. The coldest months are observed from Jun-Jul-Aug (around 18-19°C) and in the warmest months (September to January) temperatures range from 22-27°C (Fig M1-M3). Mean annual temperature has increased by 0.9°C between 1960 and 2006, with an average rate of 0.21°C per decade. This increase in temperature has been most rapid in austral summer (Dec-Jan-Feb) and slowest in Sept-Oct-Nov.

The simulated malaria season over Malawi ranges from February to July (Fig M1). The highest malaria incidence (>60%) is simulated in Mar-Apr-May (two months lag with respect to precipitation). Large malaria prevalence is simulated from April to July. The highest malaria is depicted over most of Malawi in March and April while it is greater in the northern part in May and June (Fig M4). The incidence pattern shows local minima over the southern and northern tips of the country. According to local experts in Malawi, the malaria plots are not far from reality. The 2010 Malaria Indicator Survey (2010) gives a 43.3% of malaria parasite prevalence among under five children, 46.9% for the central region and 22.8% for the north. The values of prevalence in the months March to August from the plots support these under five prevalence rates. They also support the finding that prevalence is low in the northern region.

The simulated annual mean prevalence of malaria for different driving observed datasets is shown on FigM5a. The coarse spatial resolution of the NCEP and ERAINTERIM runs still provides limited information at the country level, especially for Malawi which covers a small band in longitude. All runs agree on the fact that malaria prevalence is higher in the southern part of the country with respect to the North. The TRMM-ERA-Interim and GPCP-ERA-Interim shows local minimum of mean annual prevalence over the southern and near the northern borders of the country. All LMM simulations show that there is a large year to year variability in malaria prevalence over the northern tip of the country (north of 9°S, Fig M5b). Only TRMM-ERA-Interim and GPCP-ERA-Interim shows that the south-western border with Mozambique exhibit high malaria COV. This suggests that malaria is more likely to be epidemic in these regions. These results based on the LMM agree partly with those raised during the MARA-ARMA project (Fig M5c). The MARA risk map exhibits an endemic malaria profile in the south, the west and around the coasts of the Lake Malawi, while the northern half of the country is mainly shown as an endemic area.

The annual anomalies of rainfall, temperature and malaria prevalence are respectively shown on Fig FigM6a, FigM6b and Fig M6c. The lowest simulated malaria year (2000) is associated with exceptional cold and wet climatic conditions. The high malaria years (2001, 2003, 2007 and 2009) are not necessarily related to warmer and wetter conditions. Only 2009 was wet and slightly cooler than average. The complexity of the topography perhaps explains this change with respect to the other countries.

South Africa

South Africa is located in sub-tropical Africa and lies in between the latitude 22°S and 34°S. The country's topography is complex; much of the interior consists of extensive high plains (known as 'Veld') with an altitude of between 3,000 and 6,000 feet. The Highveld is the eastern plateau area of South Africa where lies Johannesburg at an elevation of 1750m. The country's climate is sub-tropical, but it experiences cooler temperatures than countries located at the same latitude. By contrast, the west coast from about 32° S to the border of Namibia with Angola is a desert region with a noticeably small temperature range. Fog and low cloud are frequent along this coast. The first significant rains occur in October, and the rainy season extends until the following April (Fig SA1). Most of the precipitation occurs in the eastern part of the country from November to March (Fig SA1-SA2). In the south-western tip of South Africa (Cape Town area) the wet season normally occurs during austral winter (Jun-Jul-Aug, see Fig SA2). The warmer temperatures occur from November to March while the cold season ranges from May to August (Fig SA1-SA3). The warmest month is January (with the highest averaged temperature around 26°C) while the coldest is June (with temperatures around 8°C). Mean annual temperature has increased by an average rate of 0.21°C per decade, with however large difference across the station network.

The simulated malaria season over South Africa ranges from January to May (Fig SA1). The highest malaria incidence is simulated in Feb-Mar-Apr (two months lag with respect to precipitation). Large malaria prevalence is simulated from March to June. The highest malaria is depicted over the eastern part of South Africa in February and March (Fig SA4). The simulated malaria incidence is particularly high near the south-eastern coasts of SA (from the southern border of Swaziland, including Durban, to East London), at the northern border of Swaziland (Nelspruit region) and the central / southern part of Limpopo (Fig SA4). Local experts from South Africa reported that the malaria season in South Africa is in the wet summer months from October to May. It is also seasonal, increasing in spring and summer months and decreasing in autumn. Location wise, high risk malaria areas are in Limpopo, Mpumalanga and north-eastern KwaZulu Natal while very low malaria incidences have been reported in North West and Northern Cape provinces along the Molopo and Orange rivers. The plots shown are representative of the current situation in as far as the areas where malaria occurs. Any increases in June and July could be false but last year's reports from the SA Department of Health showed early malaria cases in Limpopo that increased drastically in September. All malaria areas west of 23 degrees and south of 30 degrees

underestimates malaria (here we only modelled the impact of climate on malaria risk).

The simulated annual mean prevalence of malaria is shown on FigSA5a for different driving observed datasets. All runs agree on the fact that malaria prevalence is high along the south-eastern coasts of the country, around the Nelspruit area (northern border of Swaziland) and in the central and southern Limpopo province. All LMM simulations show that there is a large year to year variability in malaria prevalence over the north-eastern tip of the country (Fig SA5b). This suggests that malaria is more likely to be epidemic in these regions. The maximum simulated over the south-eastern coasts exhibit a weak year to year variability, denoting a more endemic profile. The malaria patterns partly agree with the MARA-ARMA maps (Fig SA5c). The MARA risk map exhibits an endemic malaria profile in the north-eastern border of the country, while the south-eastern coasts are more defined as epidemic areas (more endemic as simulated by the LMM). The LMM seems to underestimate the extension of the malaria belt in northern Limpopo.

The annual anomalies of rainfall, temperature and malaria prevalence are respectively shown on Fig FigSA6a, FigSA6b and Fig SA6c. The lowest simulated malaria years (2000 and 2006) are associated with exceptional cold and wet climatic conditions. The high malaria years (1999 and 2010) are respectively related to really warmer - slightly drier and warmer and wetter conditions. Temperature here seems to have an important role in driving the malaria anomalies, compared to what we showed for sub-Saharan countries.

4- Summary table and perspectives

Country	Rainy season	Malaria season	LMM Malaria pattern: realistic features	LMM biases, unrealistic features
Senegal	JJASO	SON (3)	Seasonality ok. Higher incidence in the south.	Malaria belt does not extend enough to the north (15°N instead of 17°N)
Ghana	MAMJJASO	JAMJJASOND (10)	Seasonality ok. Mainly endemic ok.	Problem near the coasts and populated areas.
Malawi	NDJFMA	FMAMJJ (6)	Seasonality ok. Higher incidence in the south with respect to the North.	Epidemic areas different than MARA.
South Africa	ONDJFMA	JFMAMJ (6)	Seasonality ok. High incidence over the south-eastern coasts, north of Swaziland and central southern Limpopo.	Malaria belt does not extend enough to northern Limpopo. Malaria region from model runs west of 23° and south of 30° are currently incorrect.

Perspectives:

Other malaria models (statistical / dynamical) are actually under development within the project and will be tested and compared with the LMM outputs.

In order to improve the northern location of the malaria epidemic belt (especially for Senegal) the LMM will be run with V. Ermert LMM version that showed improvements using calibrated LMM parameter settings for West Africa (Ermert et al. 2011a, 2011b).

The University of Liverpool is actually developing software (The Disease Model Cradle) that will allow the African partners to run the LMM in their local institution using meteorological station datasets. The LMM parameter settings will then be adjusted at the country level.

More malaria data will be collected during the project and this will allow a better calibration of the LMM for the targeted countries, prior to use it to provide malaria seasonal forecasts.

References

Ermert V., A. H. Fink, A.E. Jones and A. P. Morse, 2011a, Development of a new version of the Liverpool Malaria Model. I. Refining the parameter settings and mathematical formulation of basic processes based on a literature review, *Malaria Journal*, 10.35.

Ermert V., A. H. Fink, A.E. Jones and A. P. Morse, 2011b, Development of a new version of the Liverpool Malaria Model. II. Calibration and validation for West Africa, *Malaria Journal*, 10.62.

Hoshen, M. B., and A. P. Morse, 2004: A weather-driven model of malaria transmission. *Malaria J.*, **3**, 32, doi:10.1186/1475-2875-3-32.

Huffman, G.J., R.F. Adler, M. Morrissey, D.T. Bolvin, S. Curtis, R. Joyce, B. McGavock, J. Susskind, 2001: Global Precipitation at One-Degree Daily Resolution from Multi-Satellite Observations. *J. Hydrometeor.*, 2(1):36-50.

Kalnay E and co-authors (1996) The NCEP/NCAR 40-Year Reanalysis project. *Bull of Amer. Met. Soc.* 17(3): 437-471.

Morse, A. P., Doblas-Reyes, F. J., Hoshen, M. B., Hagedorn, R. and T. N. Palmer, 2005: A forecast quality assessment of an end-to-end probabilistic multi-model seasonal forecast system using a malaria model. *Tellus*, 57A:464-475.

Nájera, J. A., Kouznetsov, R. L., and C. Delacollette, 1998: *Malaria epidemics: Detection and control, forecasting and prevention*. WHO/MAL/98.1084. World Health Organization, Geneva, Switzerland. [http://www.who.int/malaria/docs/najera_epidemics/naj_toc.htm]

Uppala, S., D. Dee, S. Kobayashi, P. Berrisford, and A. Simmons (2008): Towards a climate data assimilation system: Status update of ERA-Interim, in ECMWF Newsletter, 115:12–18, European Centre for Medium-Range Weather Forecasts, Reading-UK.

WHO, 2005: *World Malaria Report 2005*. World Health Organization, Geneva, 294pp. [<http://rbm.who.int/wmr2005/html/toc.htm>]

Figures

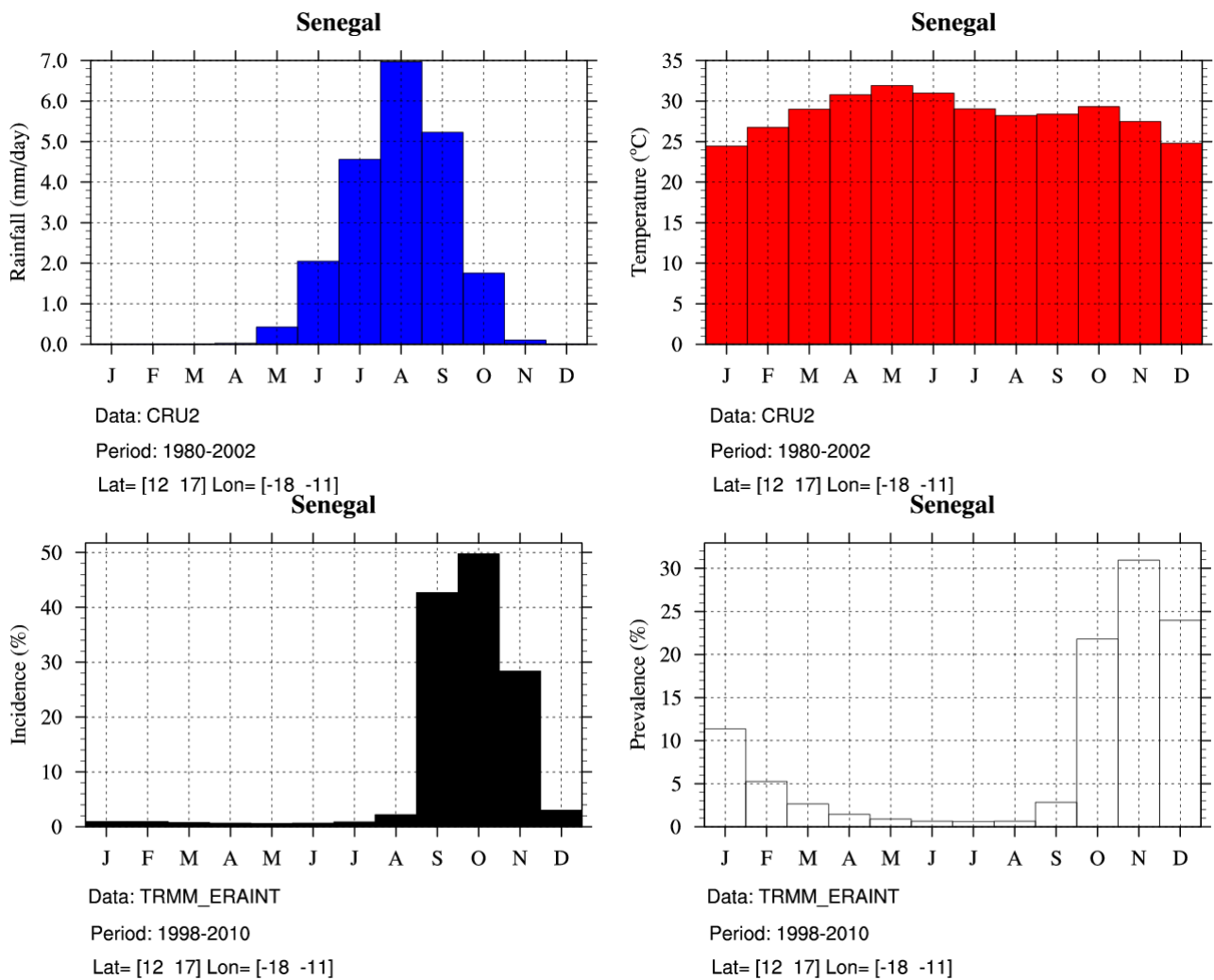


Fig S1: Upper row: Mean seasonal cycle of precipitation (left) and temperatures (right) over Senegal based on the CRUTS2.1 dataset (1980-2002). Lower row: Mean seasonal cycle of simulated malaria incidence (left) and prevalence (right). This is based on the TRMM-ERAINT simulations performed with the LMM (1998-2010).

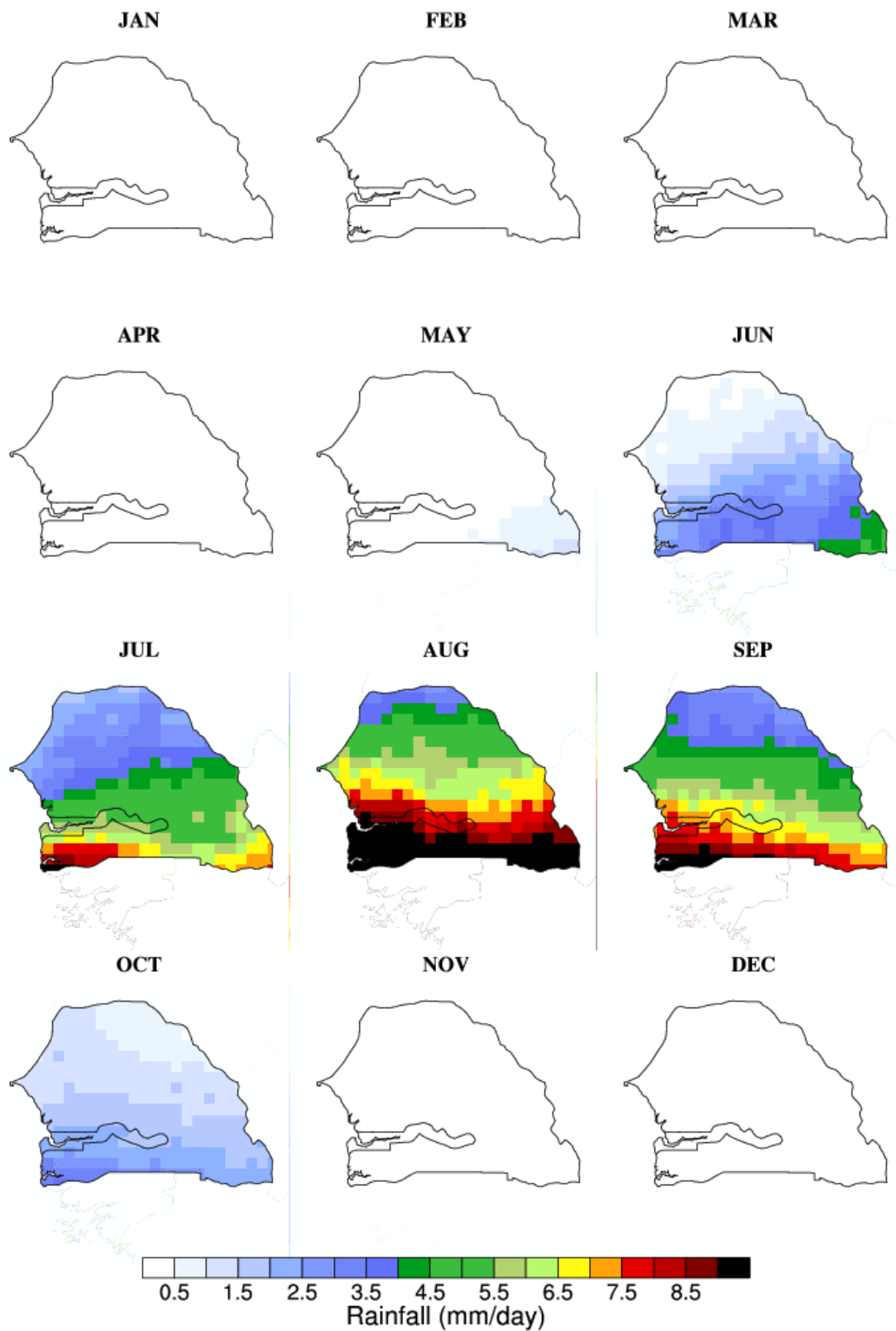


Fig S2: Mean seasonal cycle of precipitation over Senegal based on the TRMM dataset (1998-2010). Note that the CRUTS2.1 dataset shows similar patterns.

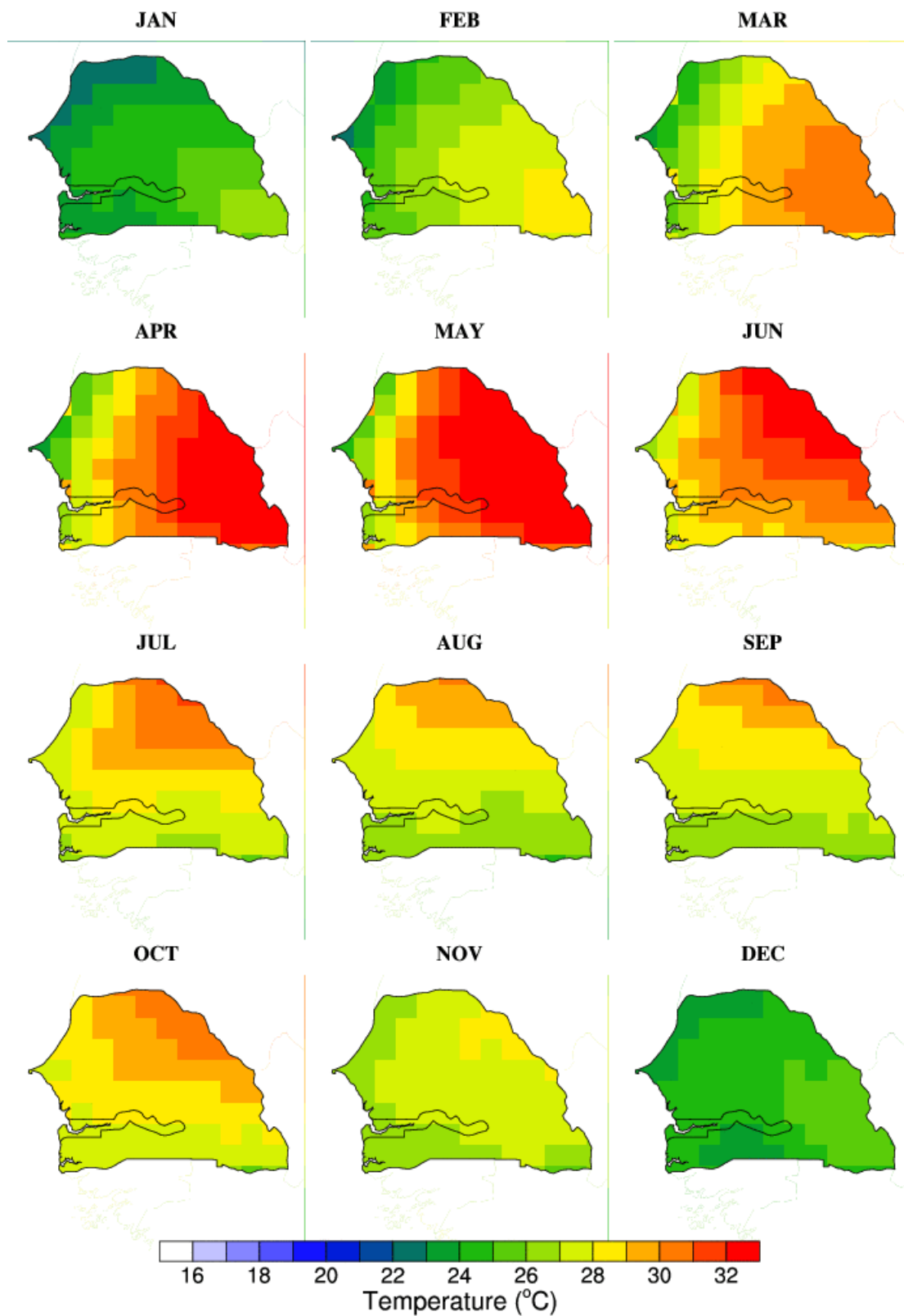


Fig S3: Mean seasonal cycle of temperature over Senegal based on the CRUTS2.1 dataset (1950-2002). Note that the ERAINTERIM dataset shows similar patterns.

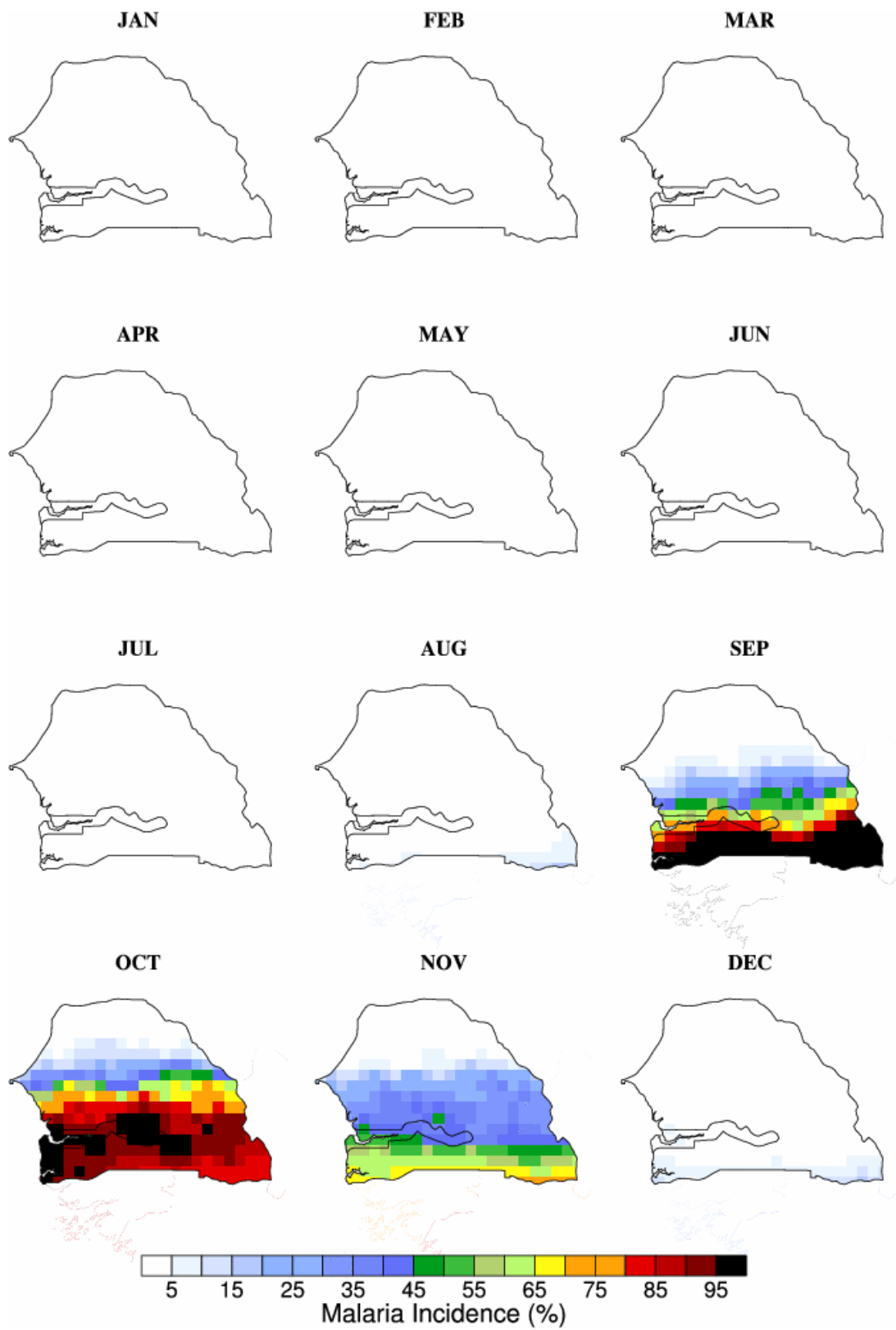


Fig S4: Mean seasonal cycle of simulated malaria incidence over Senegal based on the TRMM-ERA-Interim simulation (1998-2010).

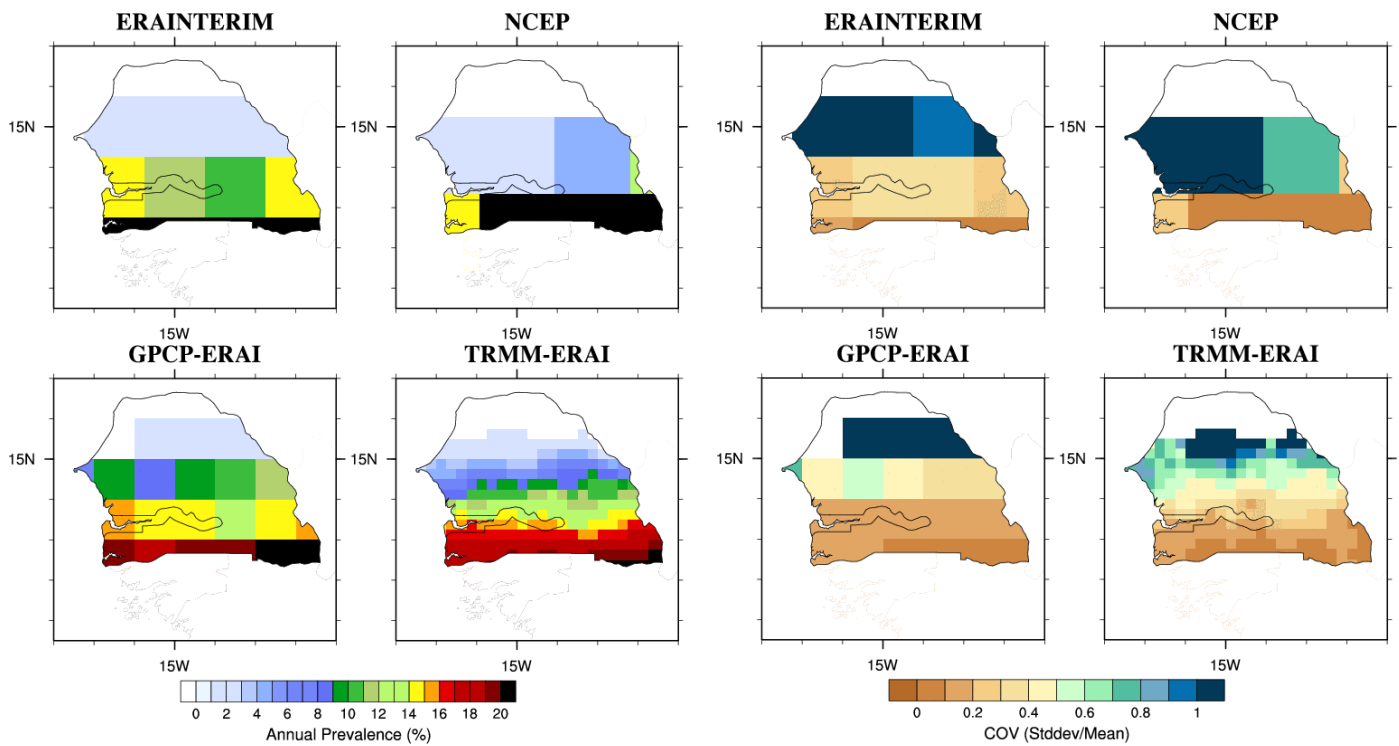


Fig S5a: Mean annual prevalence as simulated by the LMM driven by different streams of observed datasets (see table 1 for details).

Fig S5b: Coefficient of Variation (COV) based on simulated malaria prevalence. The COV is defined as the ratio between one standard deviation of the prevalence divided by the mean.

Senegal: Distribution of Endemic Malaria

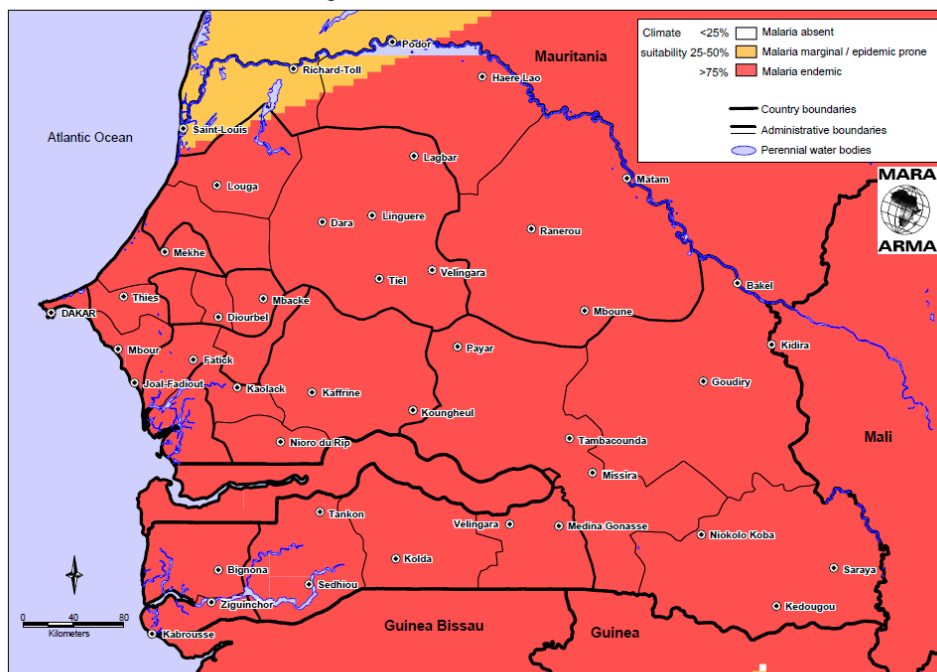


Fig S5c: Distribution of Endemic malaria based on the MARA-ARMA project.

Red, orange and white areas respectively depict where malaria is endemic, epidemic and absent.

Source: <http://www.mara.org.za/>

This map is a product of the MARA/ARMA collaboration (<http://www.mara.org.za>), July 2005, Medical Research Council, PO Box 70390, Overport, 4087, Durban, South Africa
 CORE FUNDERS of MARA/ARMA: International Development Research Centre, Canada (IDRC); The Wellcome Trust UK; South African Medical Research Council (MRC); Swiss Tropical Institute, Multilateral Initiative on Malaria (MIM) / Special Programme for Research & Training in Tropical Diseases (TDR), Roll Back Malaria (RBM).
 Malaria distribution model: Craig, M.H. et al. 1999. Parasitology Today 15: 105-111. Topographical data: African Data Sampler, WRI, http://www.igc.org/wri/sdis/maps/ads/ads_idx.htm.

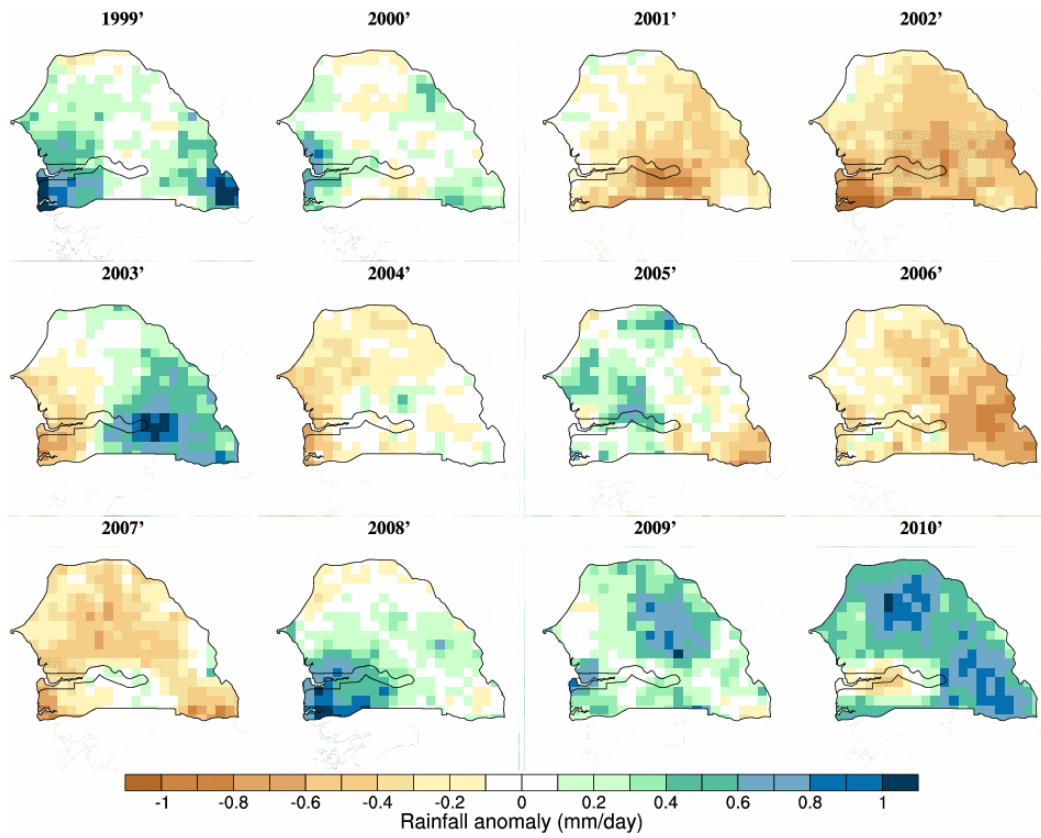


Fig S6a: Annual rainfall anomalies over Senegal (TRMM, reference climatology: 1998-2010).

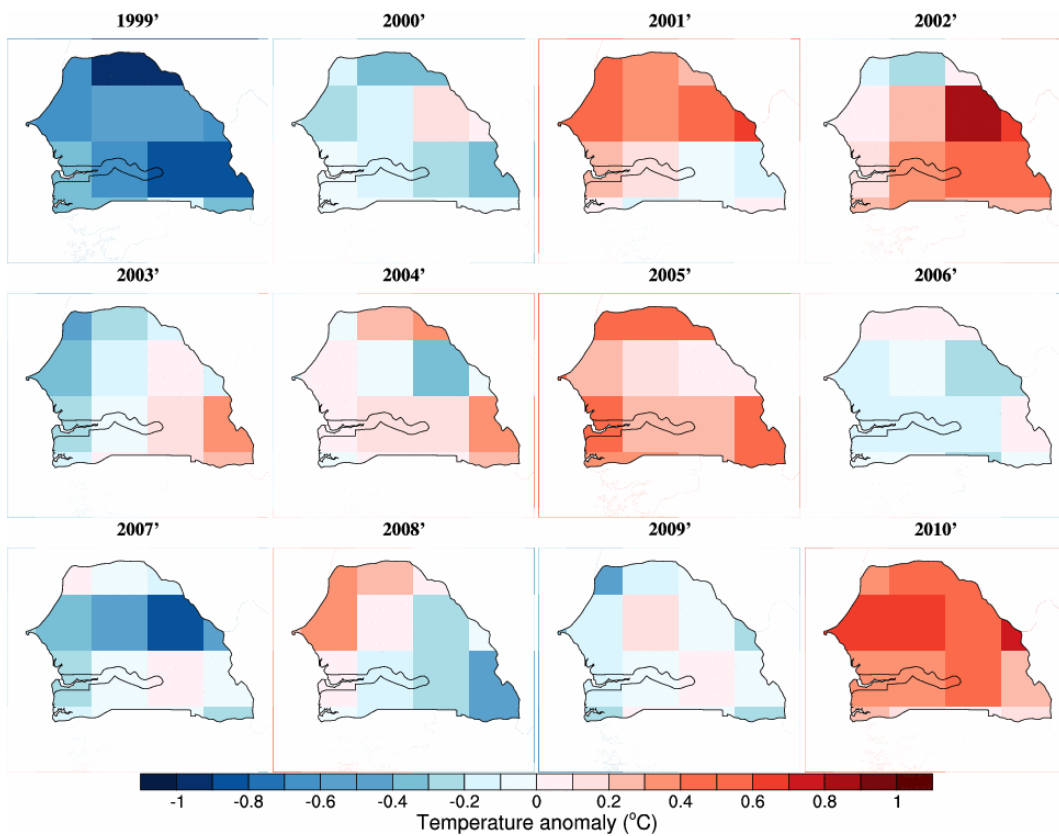


Fig S6b: Annual temperature anomalies over Senegal (ERAINTERIM, reference climatology: 1998-2010).

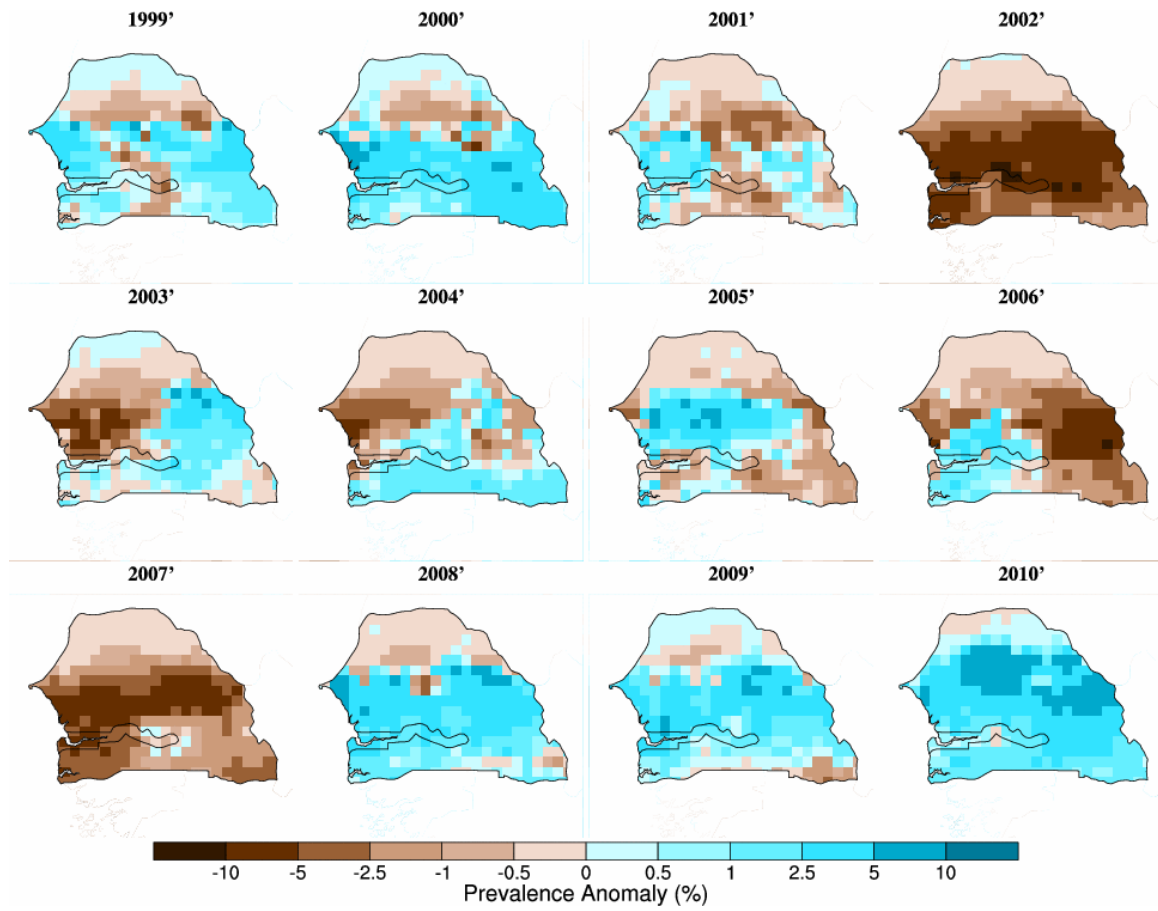
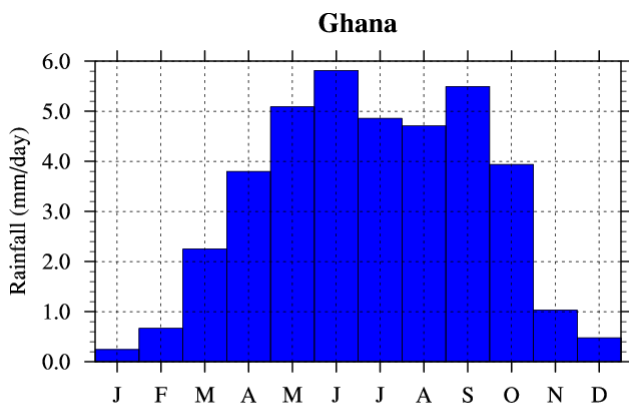
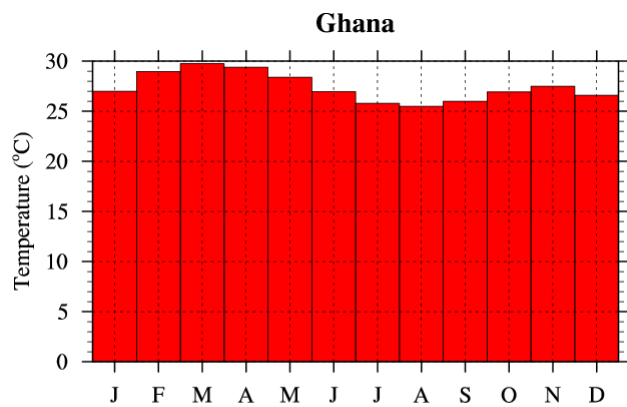


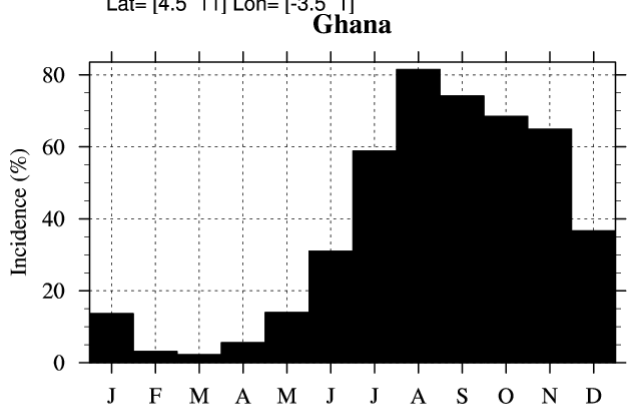
Fig S6c: Annual malaria prevalence anomalies over Senegal (TRMM-ERA-Interim, reference climatology: 1998-2010).



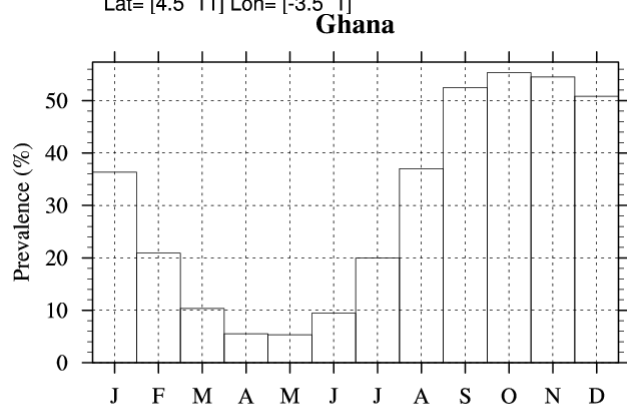
Data: CRU2
 Period: 1980-2002
 Lat= [4.5 11] Lon= [-3.5 1]



Data: CRU2
 Period: 1980-2002
 Lat= [4.5 11] Lon= [-3.5 1]



Data: TRMM_ERAIN
 Period: 1998-2010
 Lat= [4.5 11] Lon= [-3.5 1]



Data: TRMM_ERAIN
 Period: 1998-2010
 Lat= [4.5 11] Lon= [-3.5 1]

Fig G1: Upper row: Mean seasonal cycle of precipitation (left) and temperatures (right) over Ghana based on the CRUTS2.1 dataset (1980-2002). Lower row: Mean seasonal cycle of simulated malaria incidence (left) and prevalence (right). This is based on the TRMM-ERA-INT simulations performed with the LMM (1998-2010).

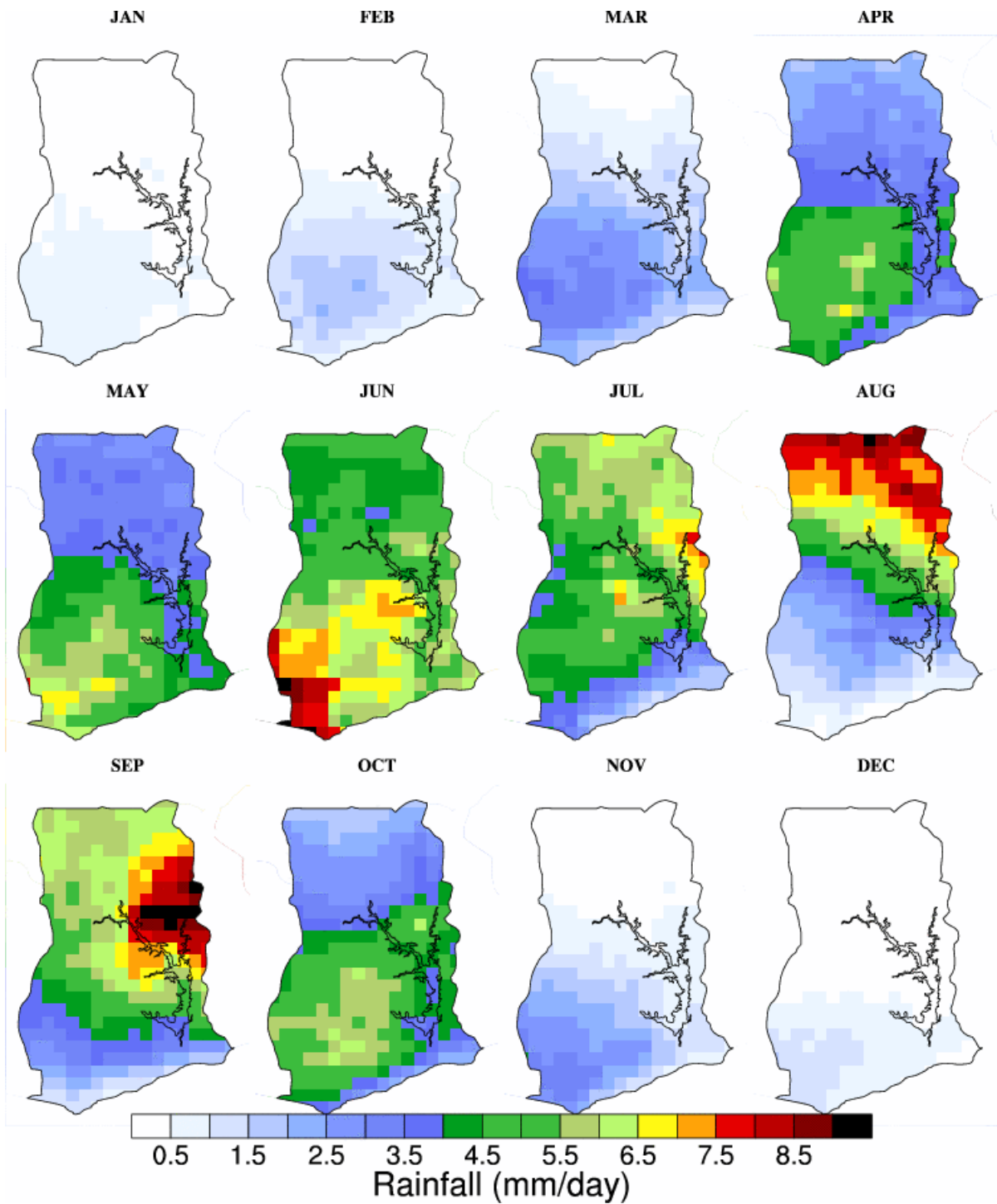


Fig G2: Mean seasonal cycle of precipitation over Ghana based on the TRMM dataset (1998-2010). Note that the CRUTS2.1 dataset shows similar patterns.

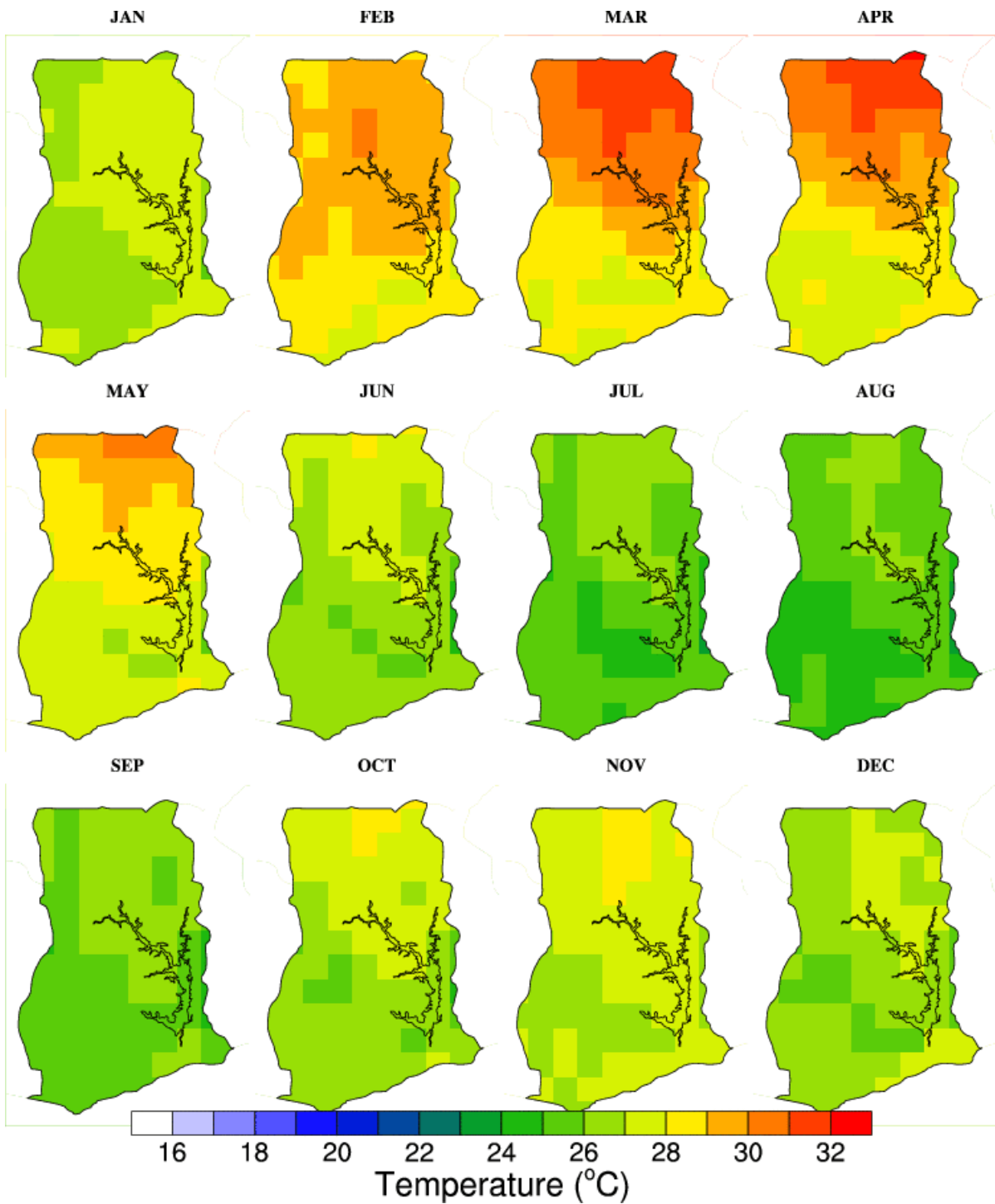


Fig G3: Mean seasonal cycle of temperature over Ghana based on the CRUTS2.1 dataset (1950-2002). Note that the ERAINTERIM dataset shows similar patterns.

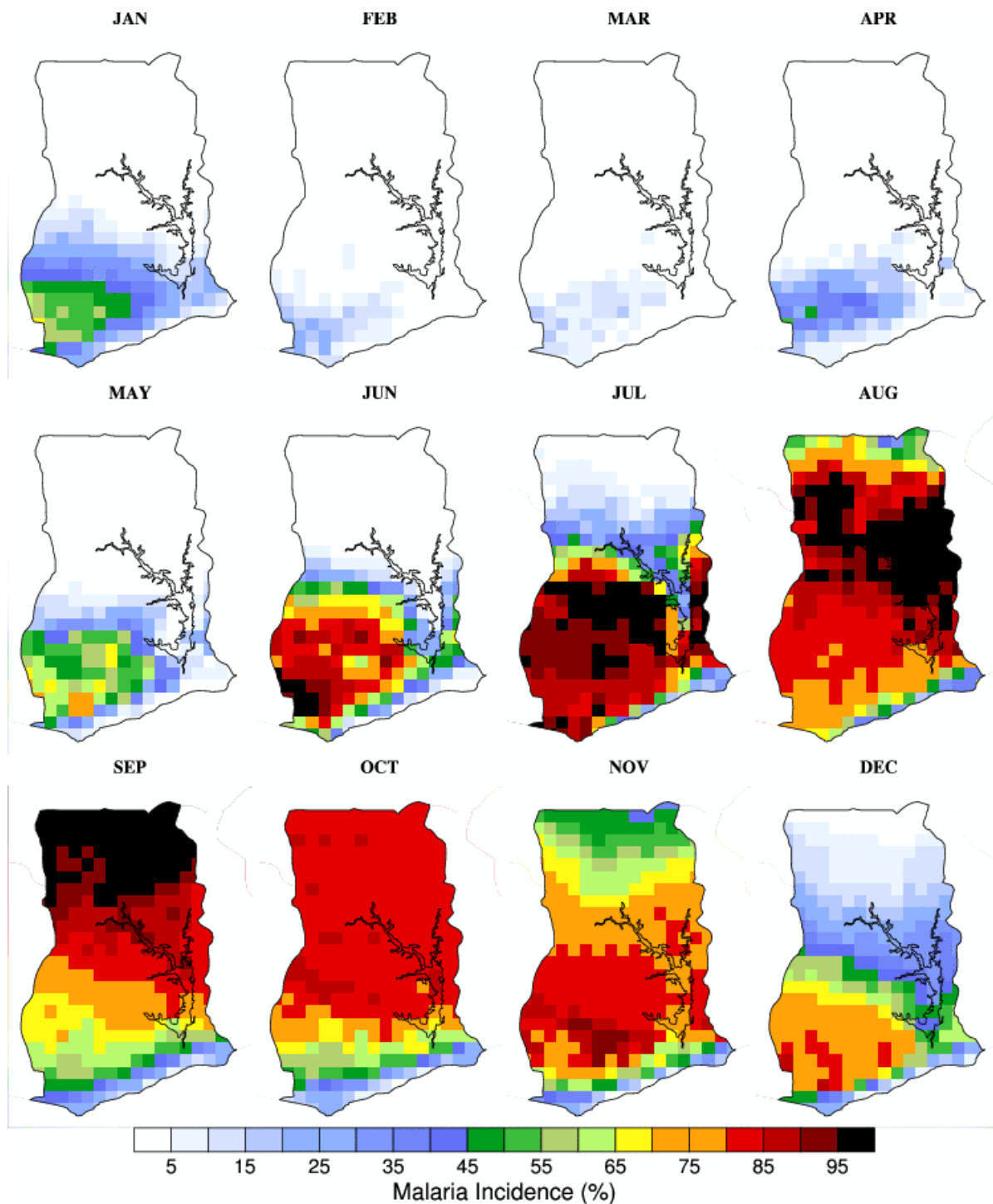


Fig G4: Mean seasonal cycle of simulated malaria incidence over Ghana based on the TRMM-ERA-Interim simulation (1998-2010).

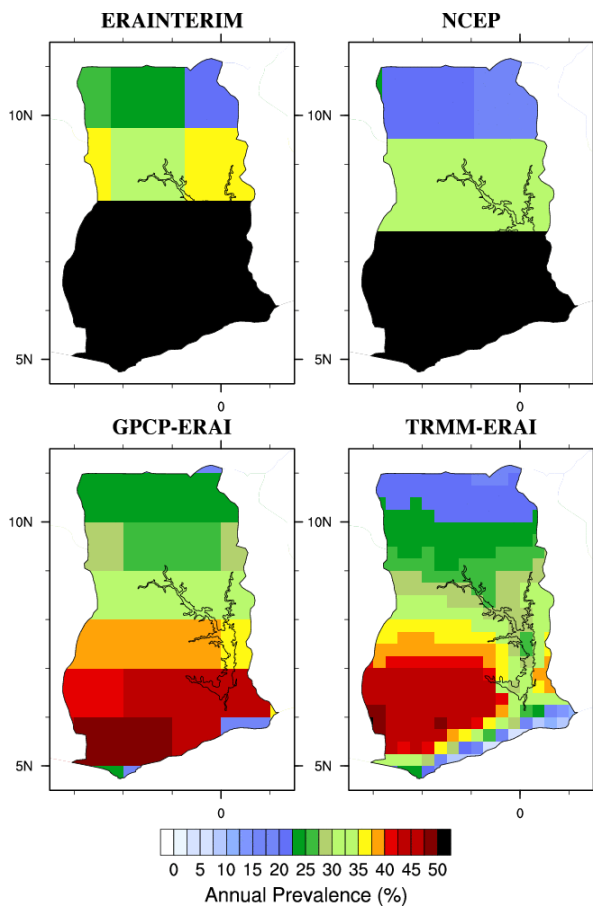


Fig G5a: Mean annual prevalence as simulated by the LMM driven by different streams of observed datasets (see table 1 for details).

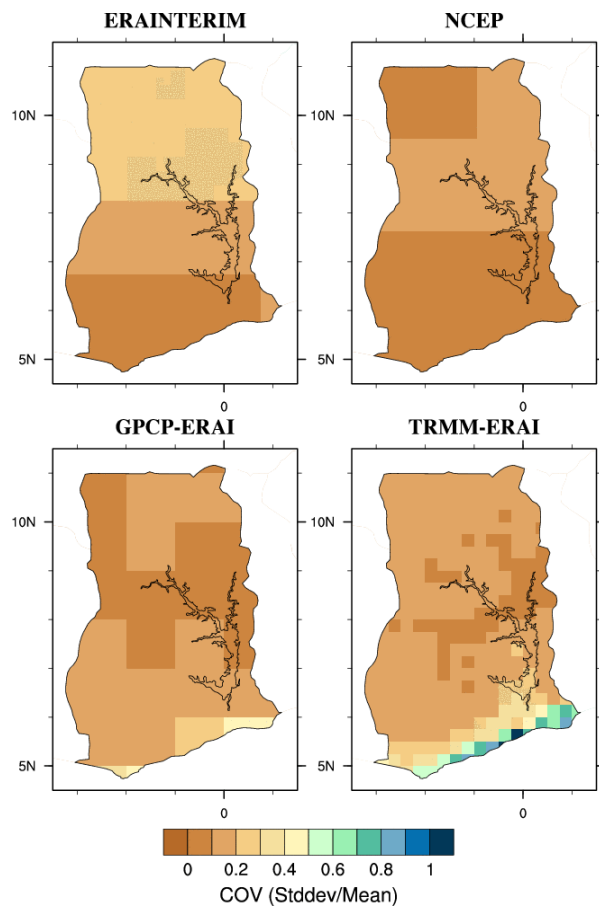


Fig G5b: Coefficient of Variation (COV) based on simulated malaria prevalence. The COV is defined as the ratio between one standard deviation of the prevalence divided by the mean.

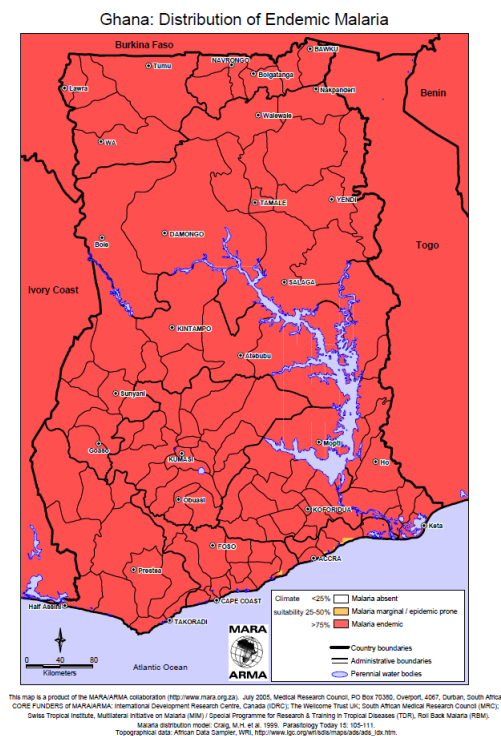


Fig G5c: Distribution of Endemic malaria based on the MARA-ARMA project.

Red, orange and white areas respectively depict where malaria is endemic, epidemic/marginal and absent.

Source:
<http://www.mara.org.za/>

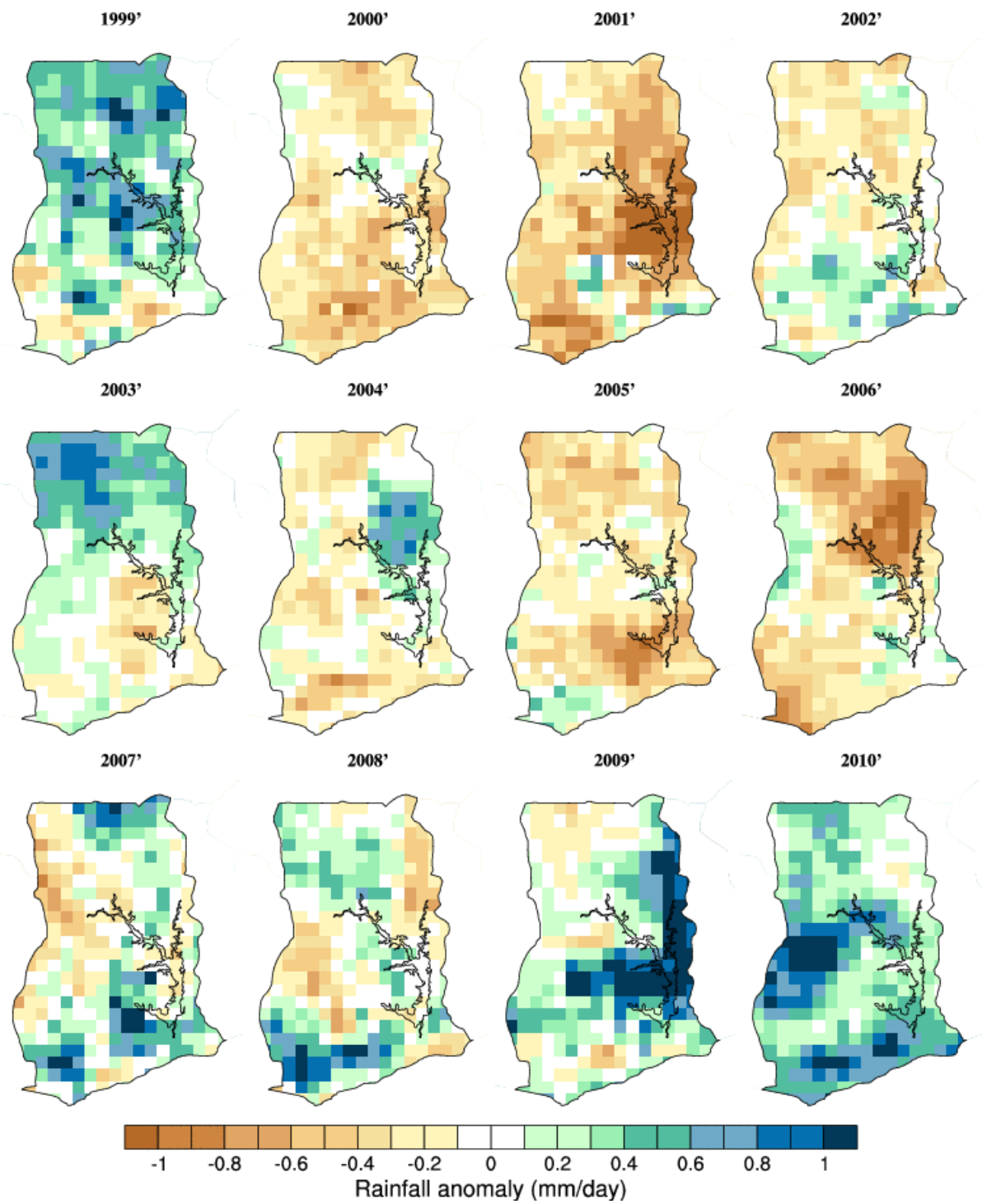


Fig G6a: Annual rainfall anomalies over Ghana (TRMM, reference climatology: 1998-2010).

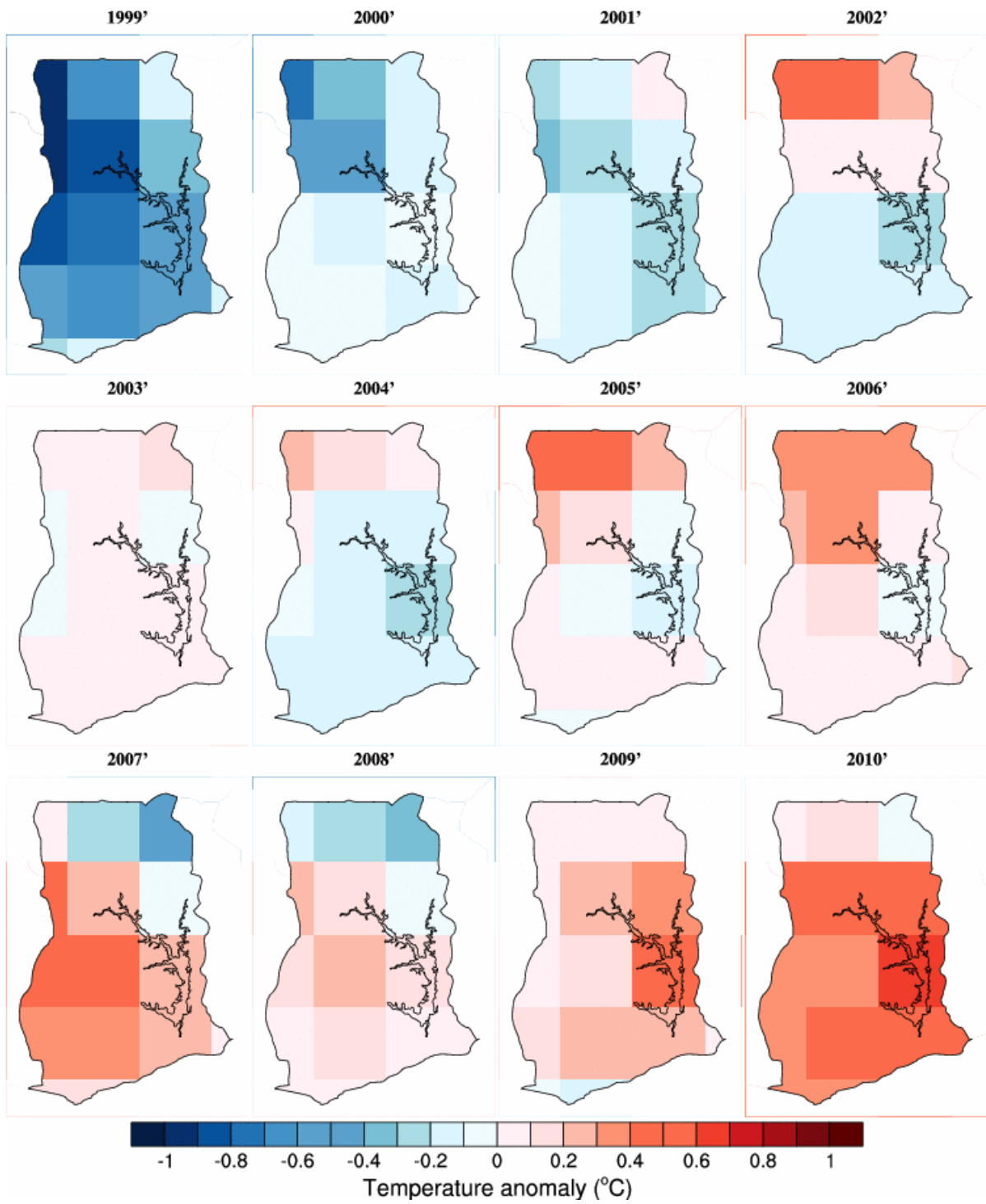


Fig G6b: Annual temperature anomalies over Ghana (ERAINTERIM, reference climatology: 1998-2010).

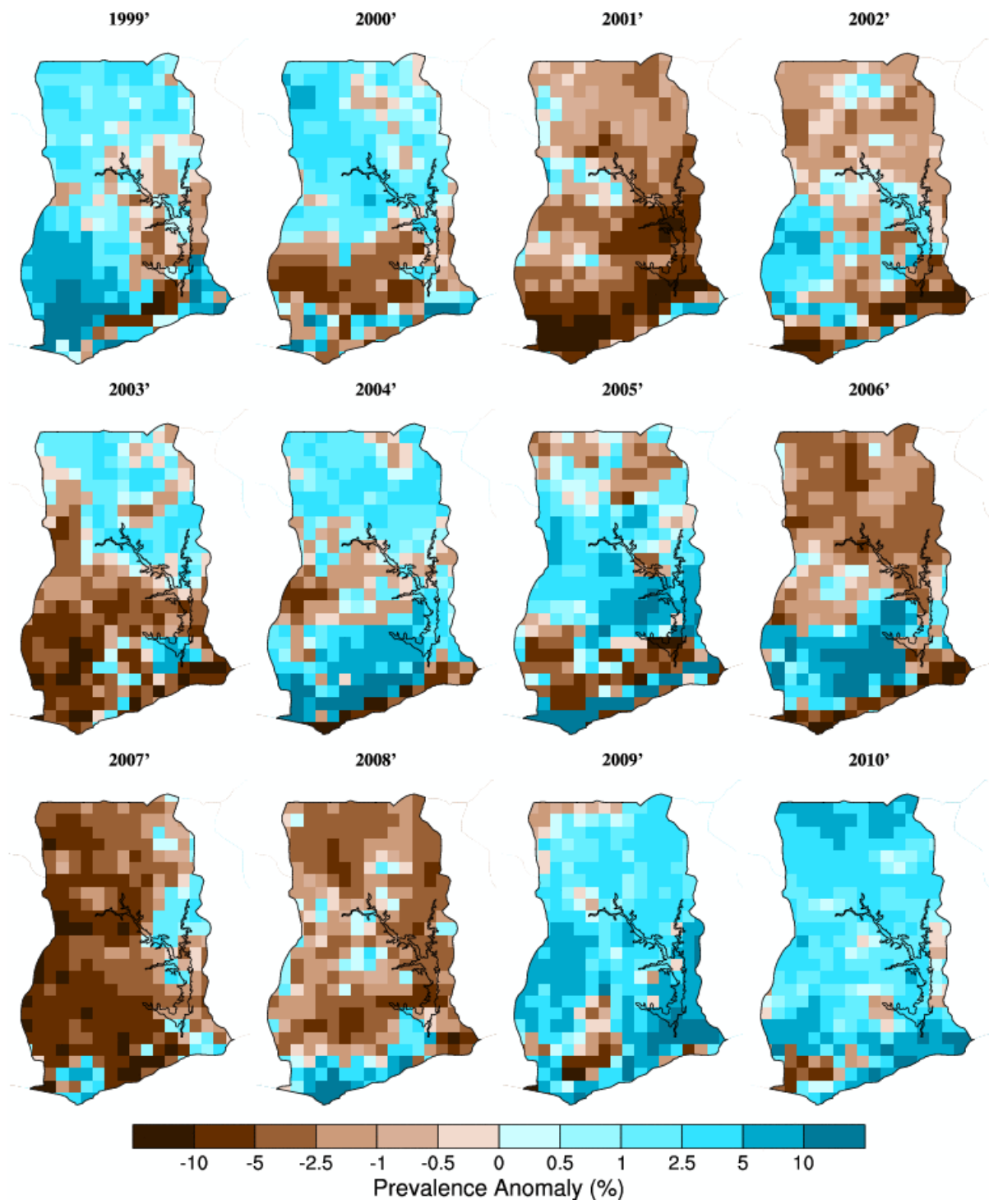
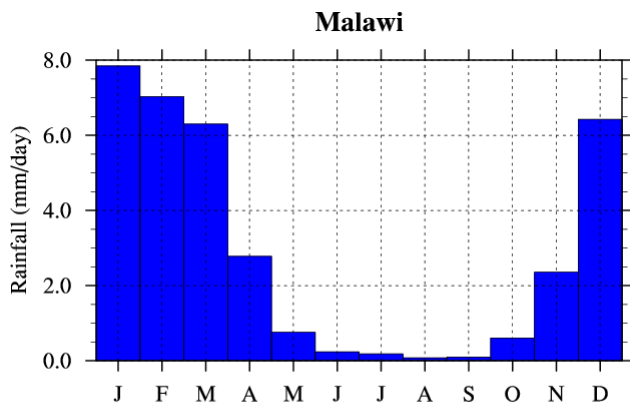
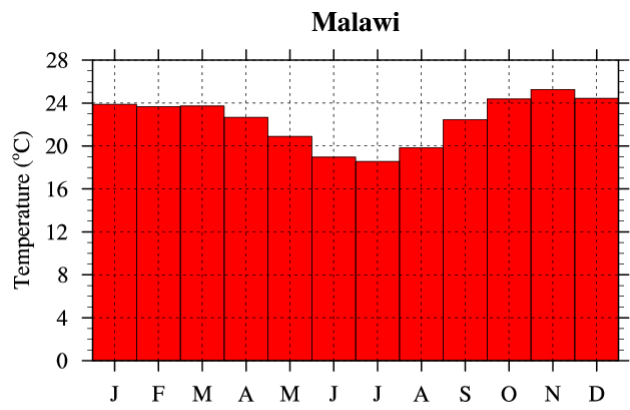


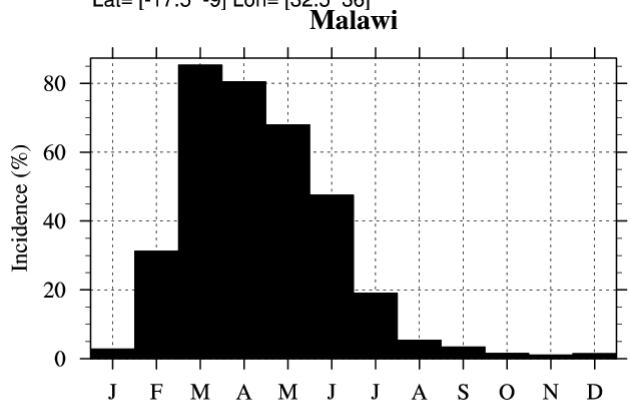
Fig G6c: Annual malaria prevalence anomalies over Ghana (TRMM-ERA-Interim, reference climatology: 1998-2010).



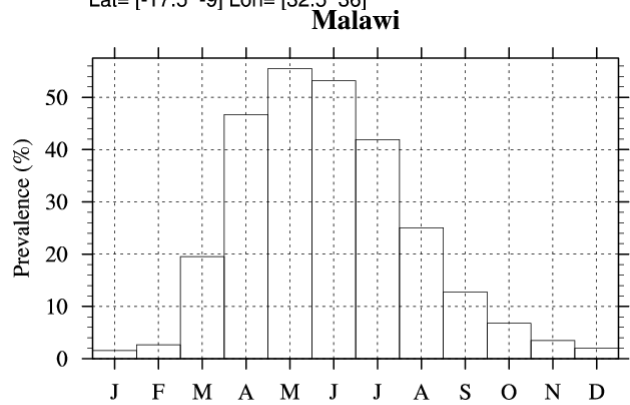
Data: CRU2
 Period: 1980-2002
 Lat= [-17.5 -9] Lon= [32.5 36]



Data: CRU2
 Period: 1980-2002
 Lat= [-17.5 -9] Lon= [32.5 36]



Data: TRMM ERAINT
 Period: 1998-2010
 Lat= [-17.5 -9] Lon= [32.5 36]



Data: TRMM ERAINT
 Period: 1998-2010
 Lat= [-17.5 -9] Lon= [32.5 36]

Fig M1: Upper row: Mean seasonal cycle of precipitation (left) and temperatures (right) over Malawi based on the CRUTS2.1 dataset (1980-2002). Lower row: Mean seasonal cycle of simulated malaria incidence (left) and prevalence (right). This is based on the TRMM-ERAINT simulations performed with the LMM (1998-2010).

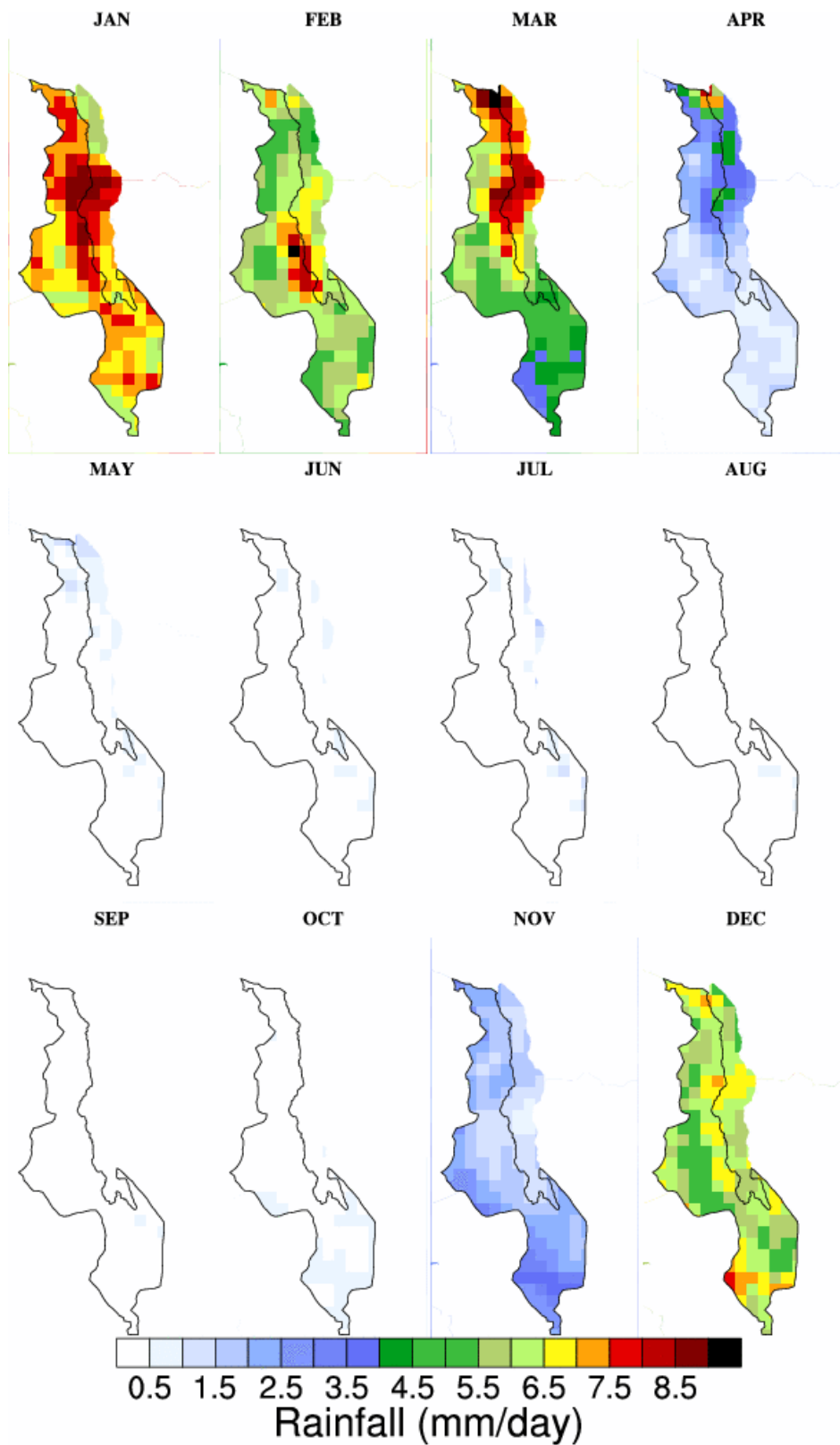


Fig M2: Mean seasonal cycle of precipitation over Malawi based on the TRMM dataset (1998-2010). Note that the CRUTS2.1 dataset shows similar patterns.

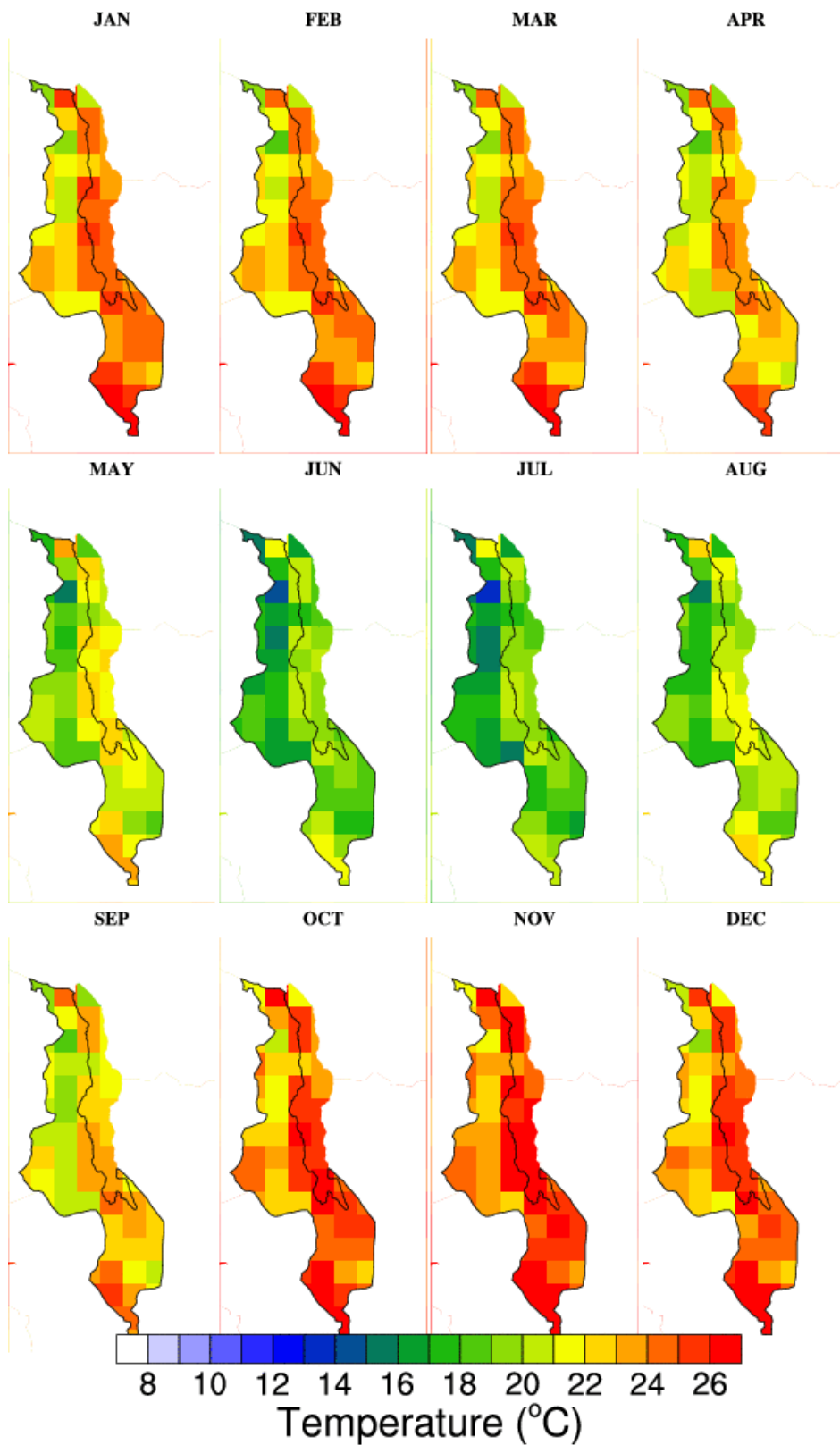


Fig M3: Mean seasonal cycle of temperature over Malawi based on the CRUTS2.1 dataset (1950-2002). Note that the ERAINTERIM dataset shows similar patterns.

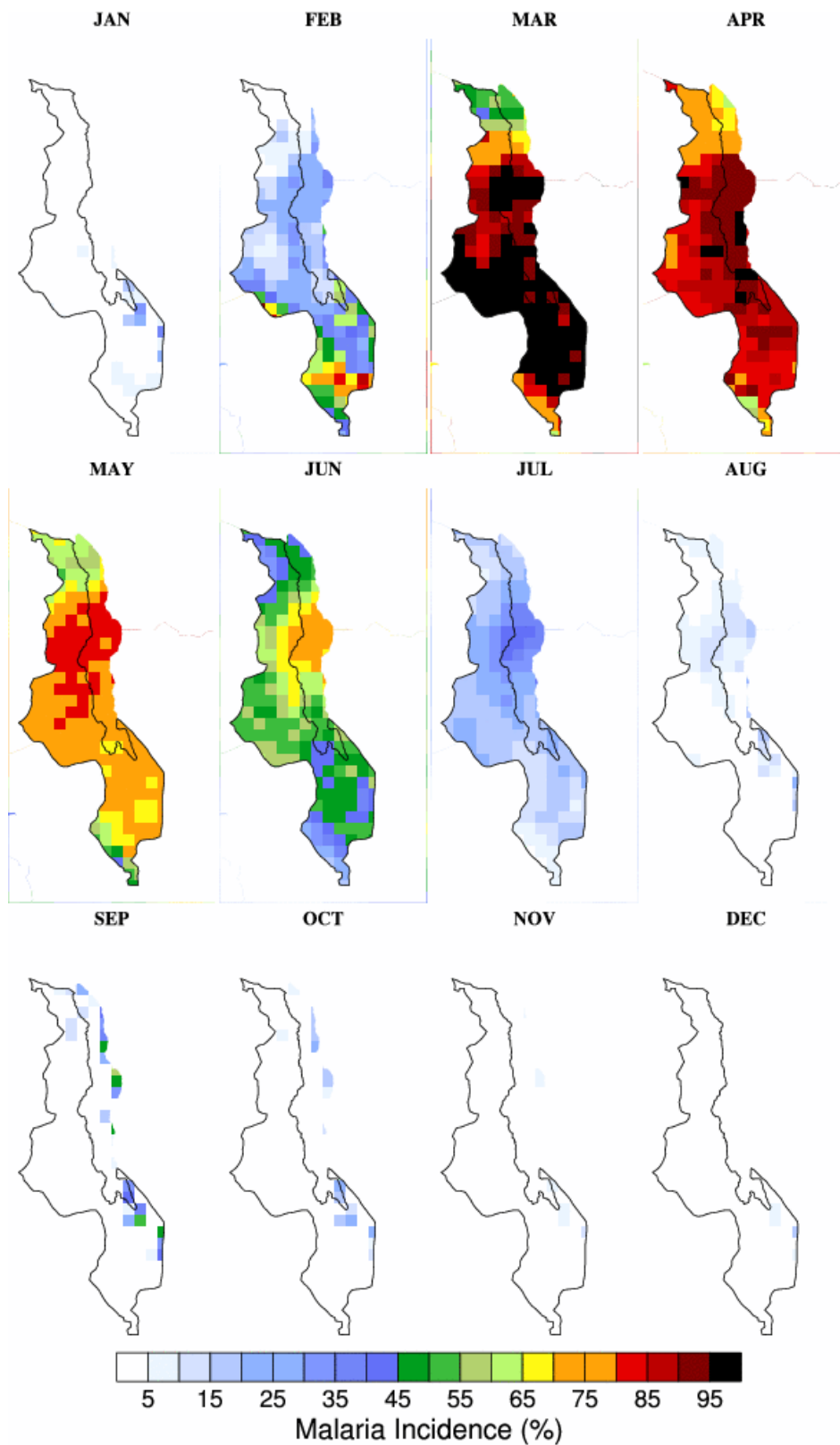


Fig M4: Mean seasonal cycle of simulated malaria incidence over Malawi based on the TRMM-ERA-Interim simulation (1998-2010).

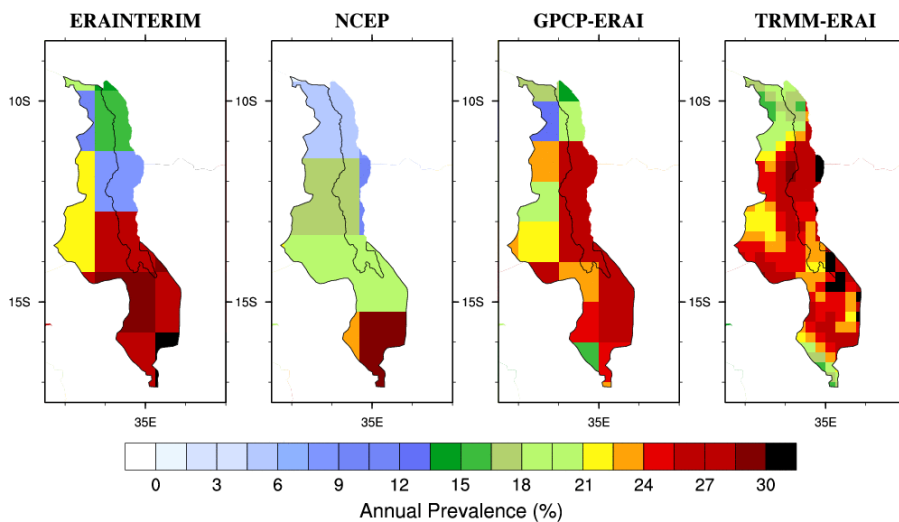


Fig M5a: Mean annual prevalence as simulated by the LMM driven by different streams of observed datasets (see table 1 for details).

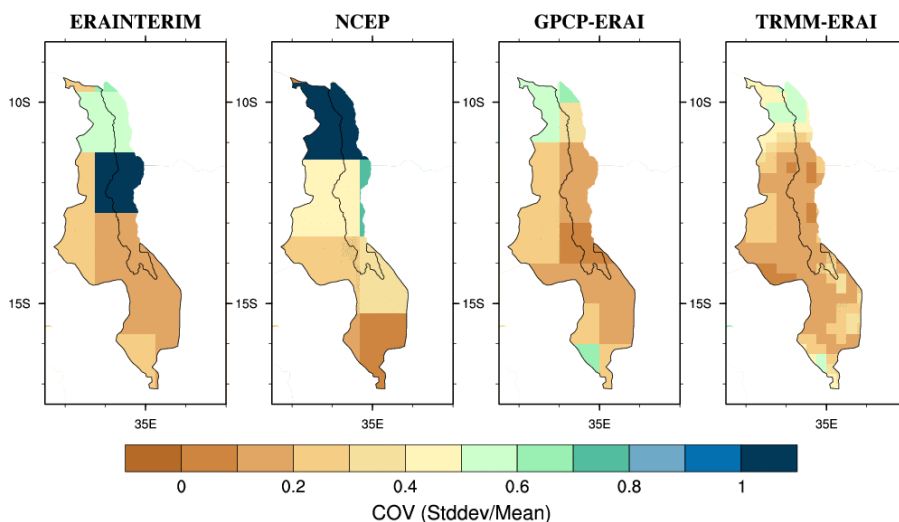


Fig M5b: Coefficient of Variation (COV) based on simulated malaria prevalence. The COV is defined as the ratio between one standard deviation of the prevalence divided by the mean.

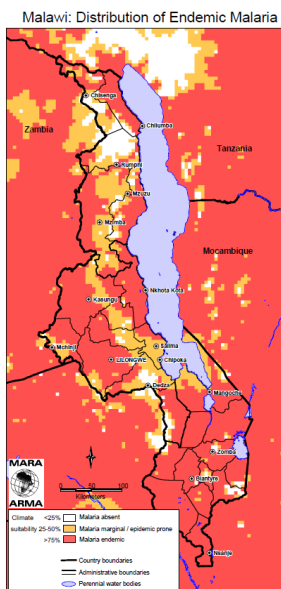


Fig M5c: Distribution of Endemic malaria based on the MARA-ARMA project.

Red, orange and white areas respectively depict where malaria is endemic, epidemic/marginal and absent.

Source:

<http://www.mara.org.za/>

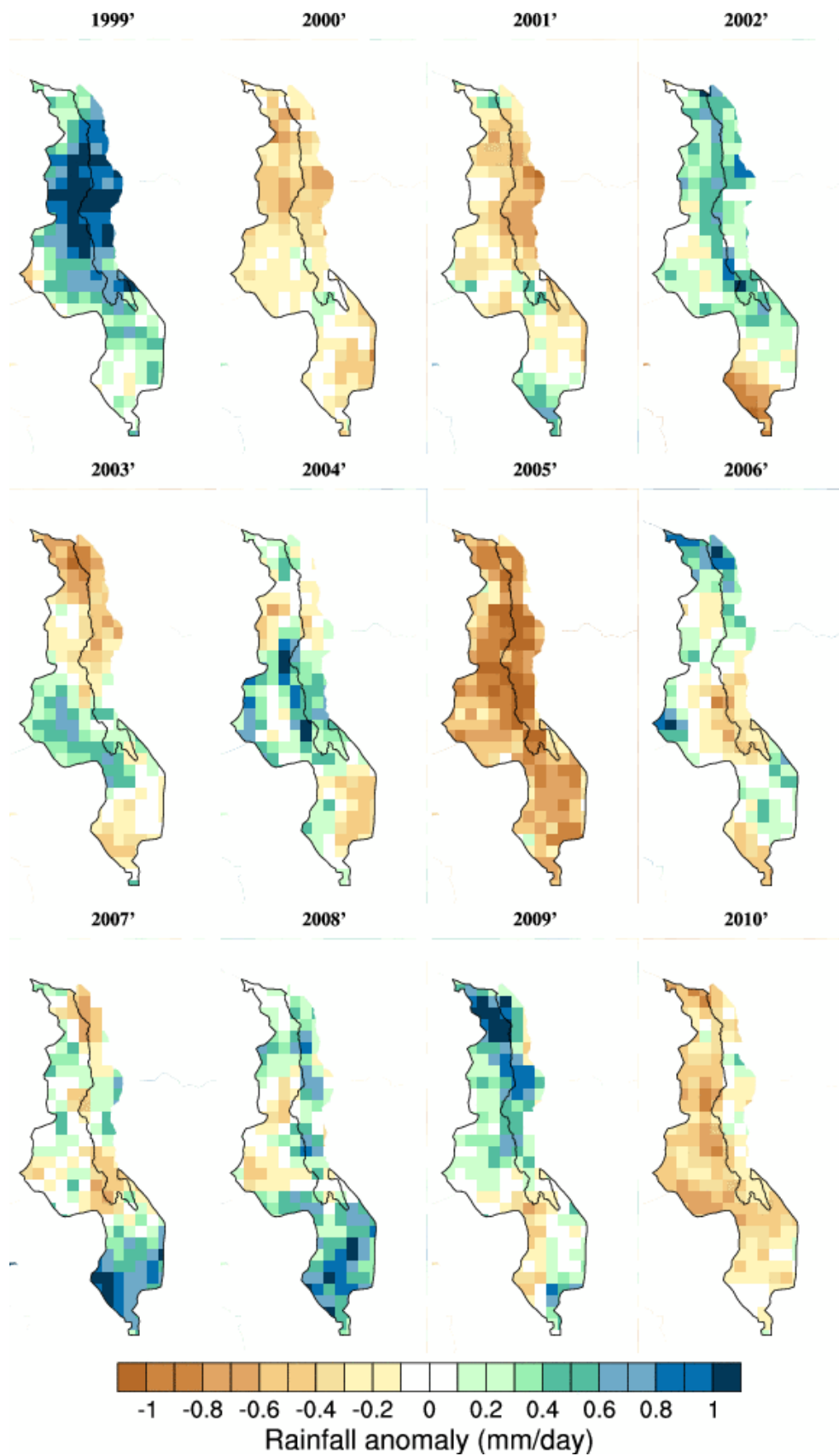


Fig M6a: Annual rainfall anomalies over Malawi (TRMM, reference climatology: 1998-2010).

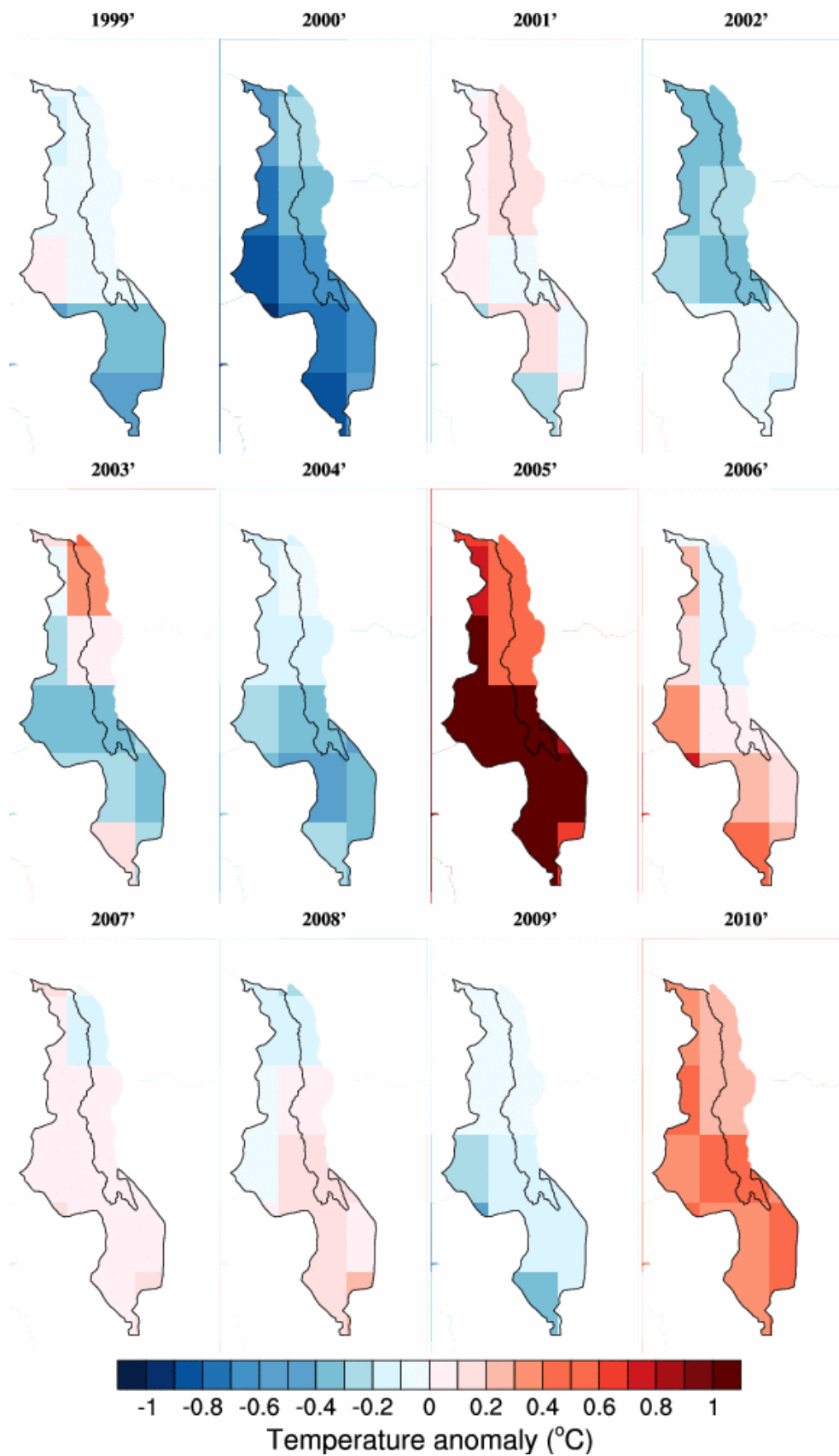


Fig M6b: Annual temperature anomalies over Malawi (ERAINTERIM, reference climatology: 1998-2010).

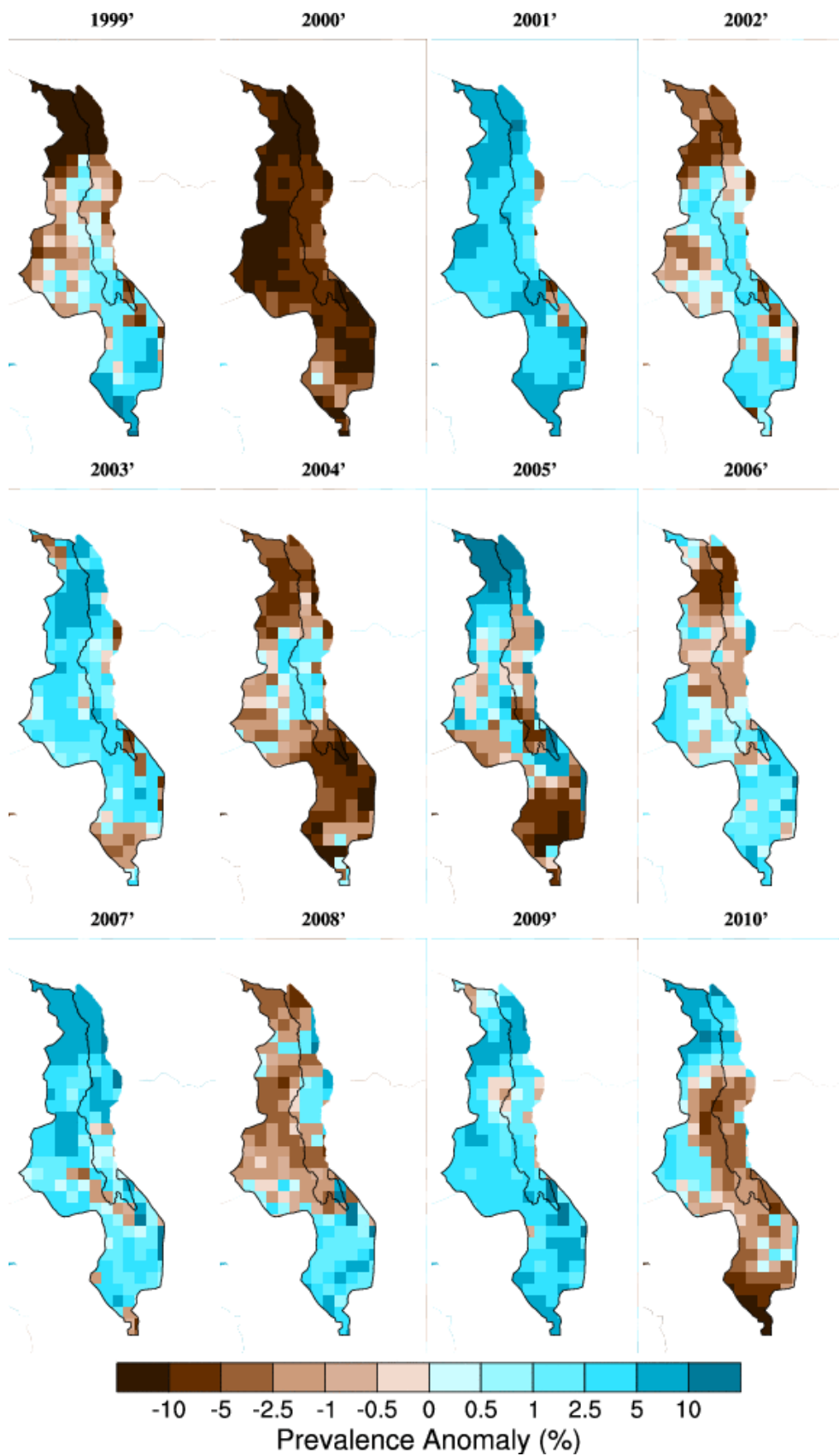
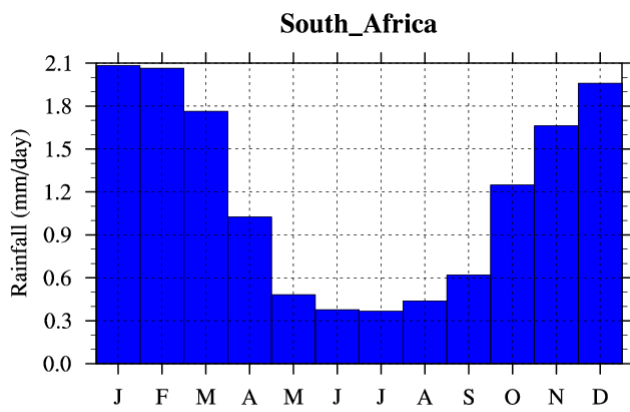
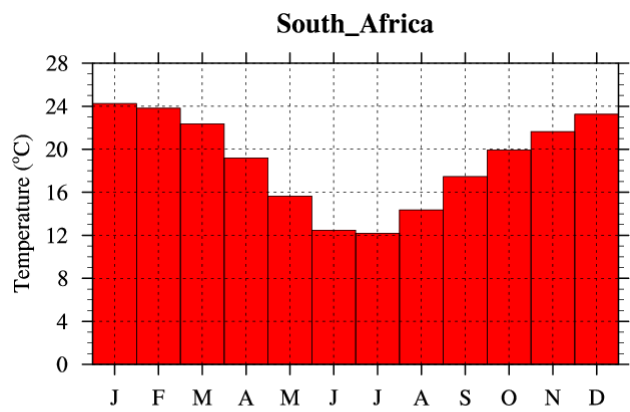


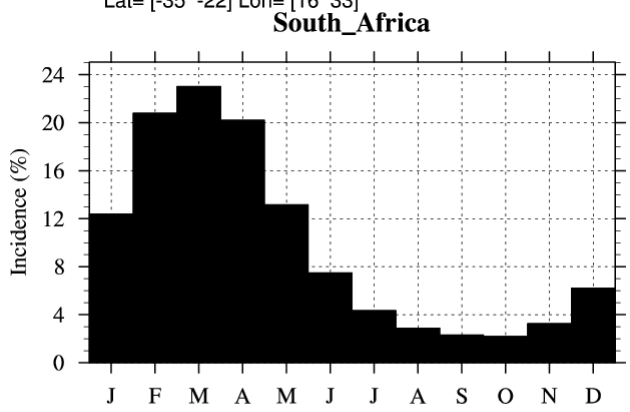
Fig M6c: Annual malaria prevalence anomalies over Malawi (TRMM-ERAI, reference climatology: 1998-2010).



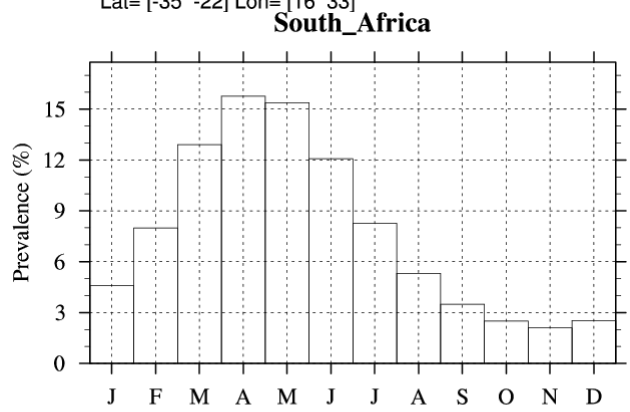
Data: CRU2
 Period: 1980-2002
 Lat= [-35 -22] Lon=[16 33]



Data: CRU2
 Period: 1980-2002
 Lat= [-35 -22] Lon=[16 33]



Data: TRMM ERAINT
 Period: 1998-2010
 Lat= [-35 -22] Lon=[16 33]



Data: TRMM ERAINT
 Period: 1998-2010
 Lat= [-35 -22] Lon=[16 33]

Fig SA1: Upper row: Mean seasonal cycle of precipitation (left) and temperatures (right) over South Africa based on the CRUTS2.1 dataset (1980-2002). Lower row: Mean seasonal cycle of simulated malaria incidence (left) and prevalence (right). This is based on the TRMM-ERAINT simulations performed with the LMM (1998-2010).

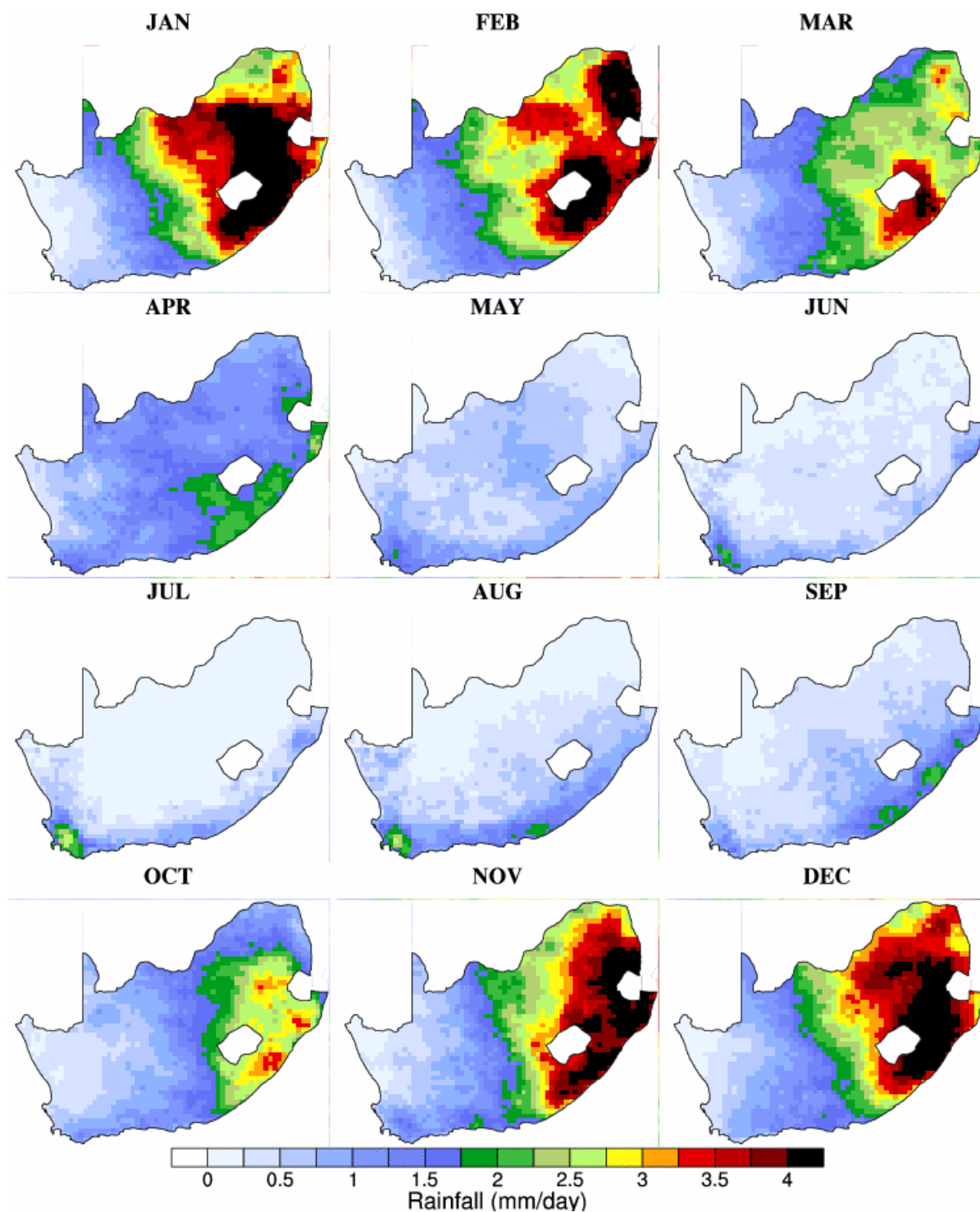


Fig SA2: Mean seasonal cycle of precipitation over South Africa based on the TRMM dataset (1998-2010). Note that the CRUTS2.1 dataset shows similar patterns.

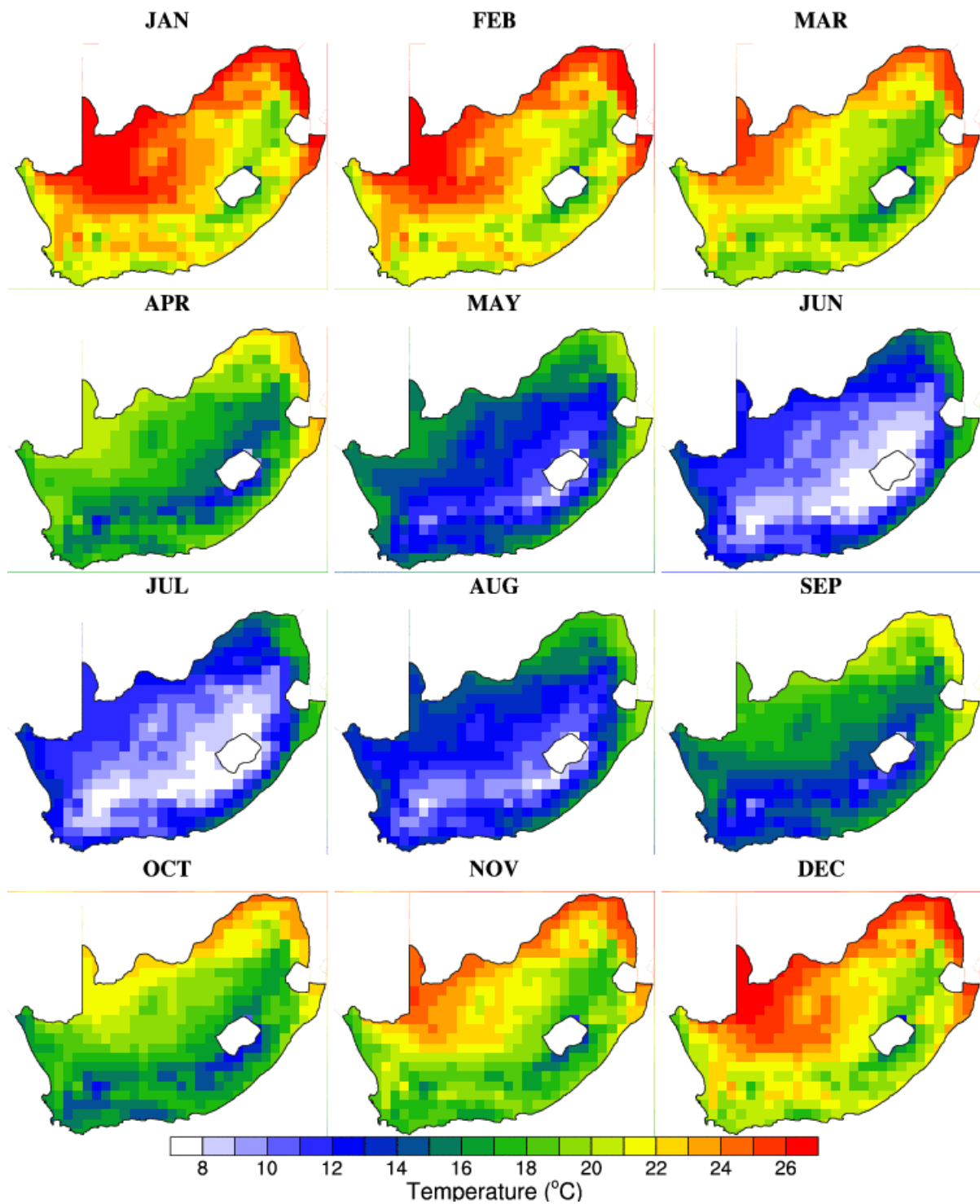


Fig SA3: Mean seasonal cycle of temperature over South Africa based on the CRUTS2.1 dataset (1950-2002). Note that the ERAINTERIM dataset shows similar patterns.

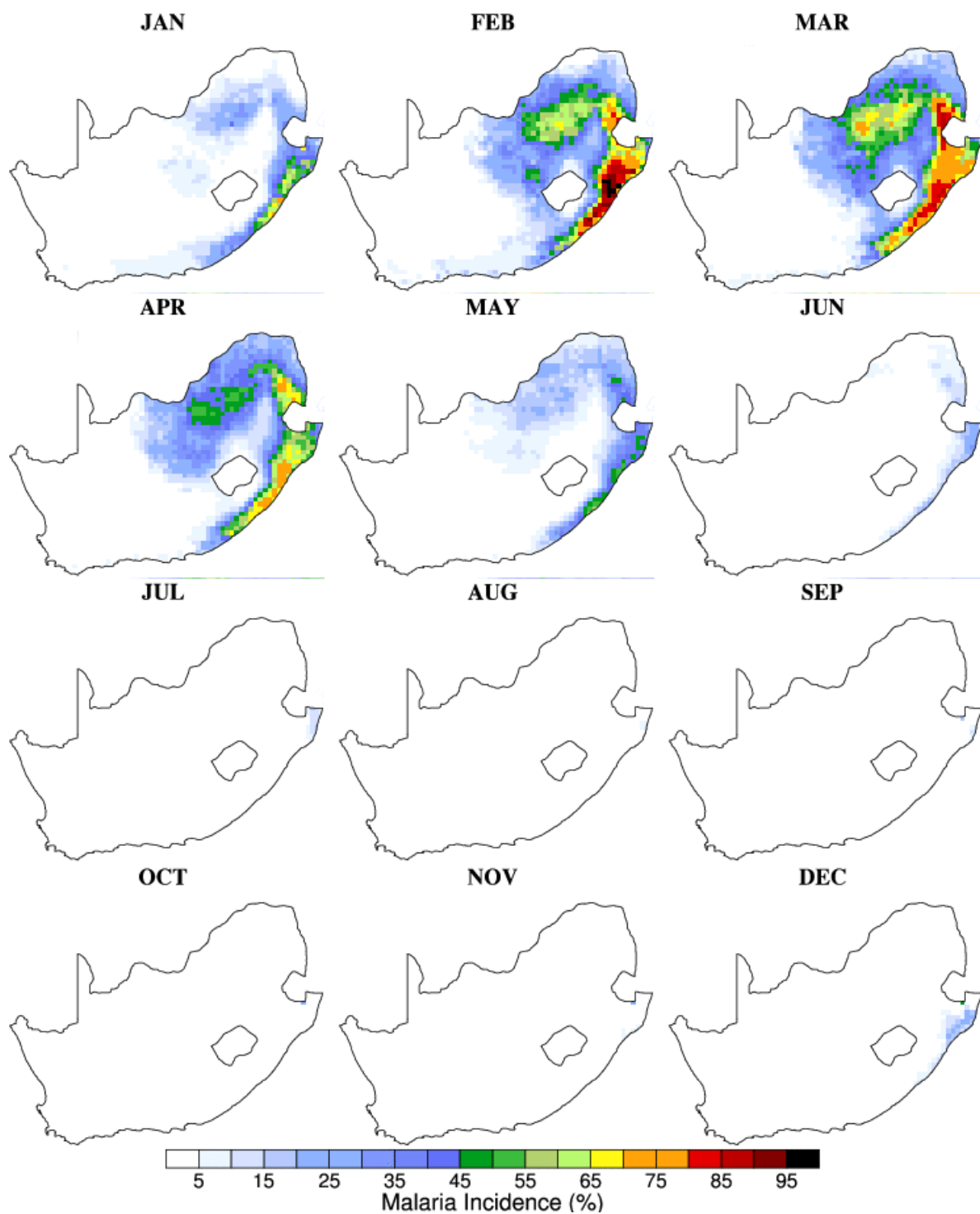


Fig SA4: Mean seasonal cycle of simulated malaria incidence over South Africa based on the TRMM-ERA-Interim simulation (1998-2010).

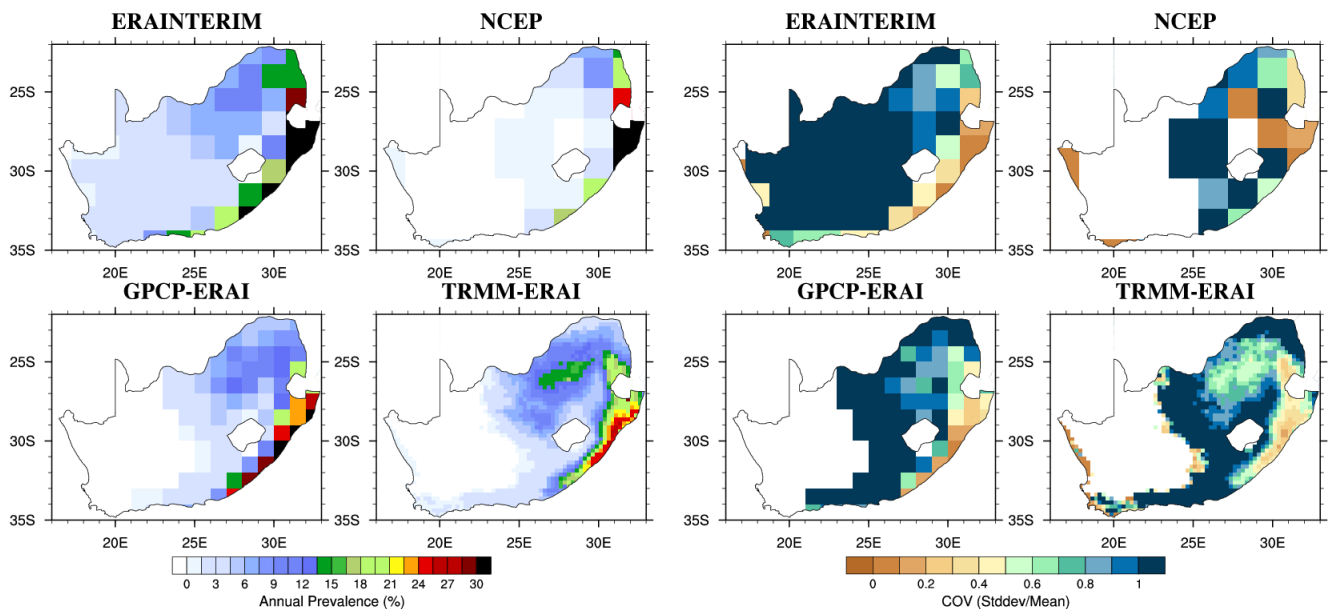


Fig SA5a: Mean annual prevalence as simulated by the LMM driven by different streams of observed datasets (see table 1 for details).

Fig SA5b: Coefficient of Variation (COV) based on simulated malaria prevalence. The COV is defined as the ratio between one standard deviation of the prevalence divided by the mean.

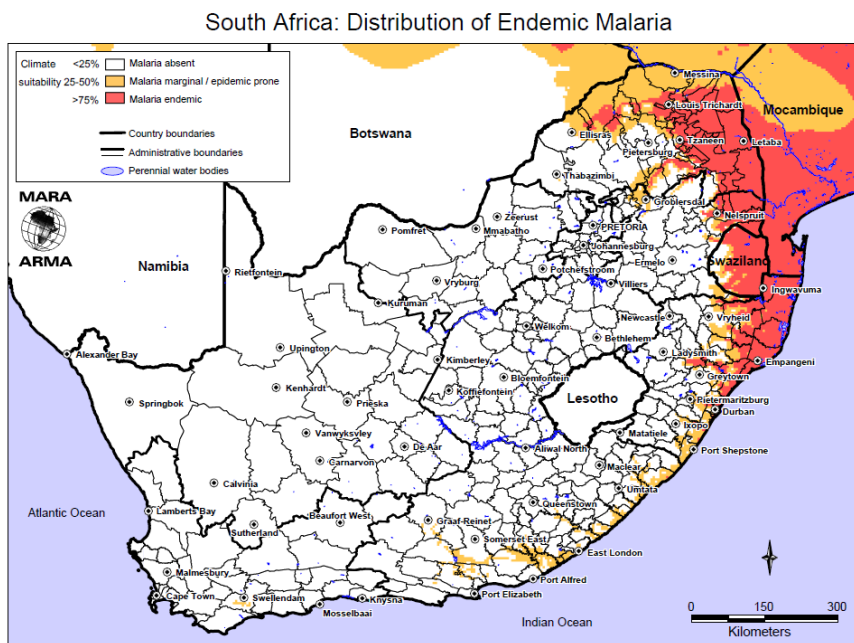


Fig SA5c: Distribution of Endemic malaria based on the MARA-ARMA project.

Red, orange and white areas respectively depict where malaria is endemic, epidemic/marginal and absent.

Source:
<http://www.mara.org.za/>

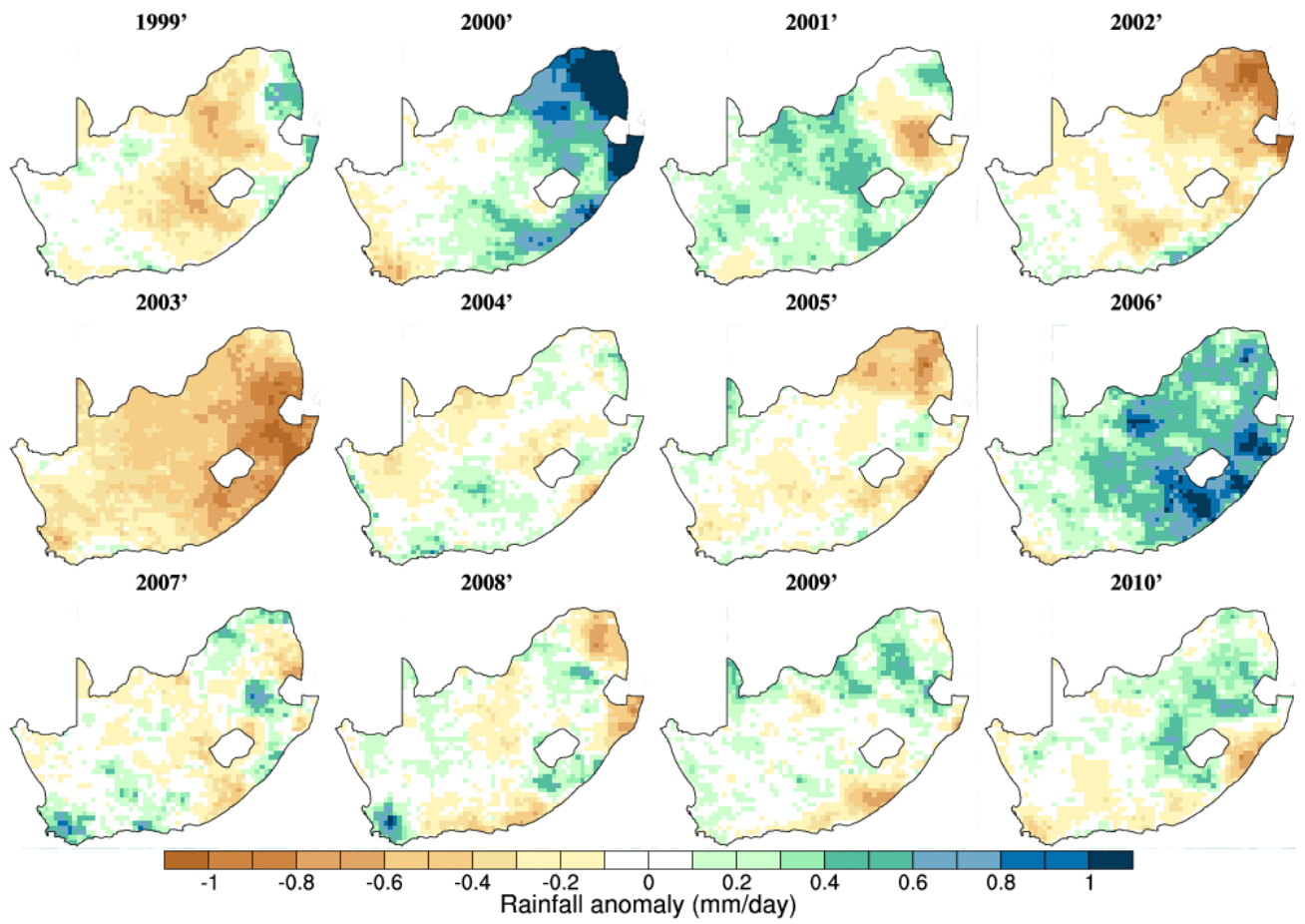


Fig SA6a: Annual rainfall anomalies over South Africa (TRMM, reference climatology: 1998-2010).

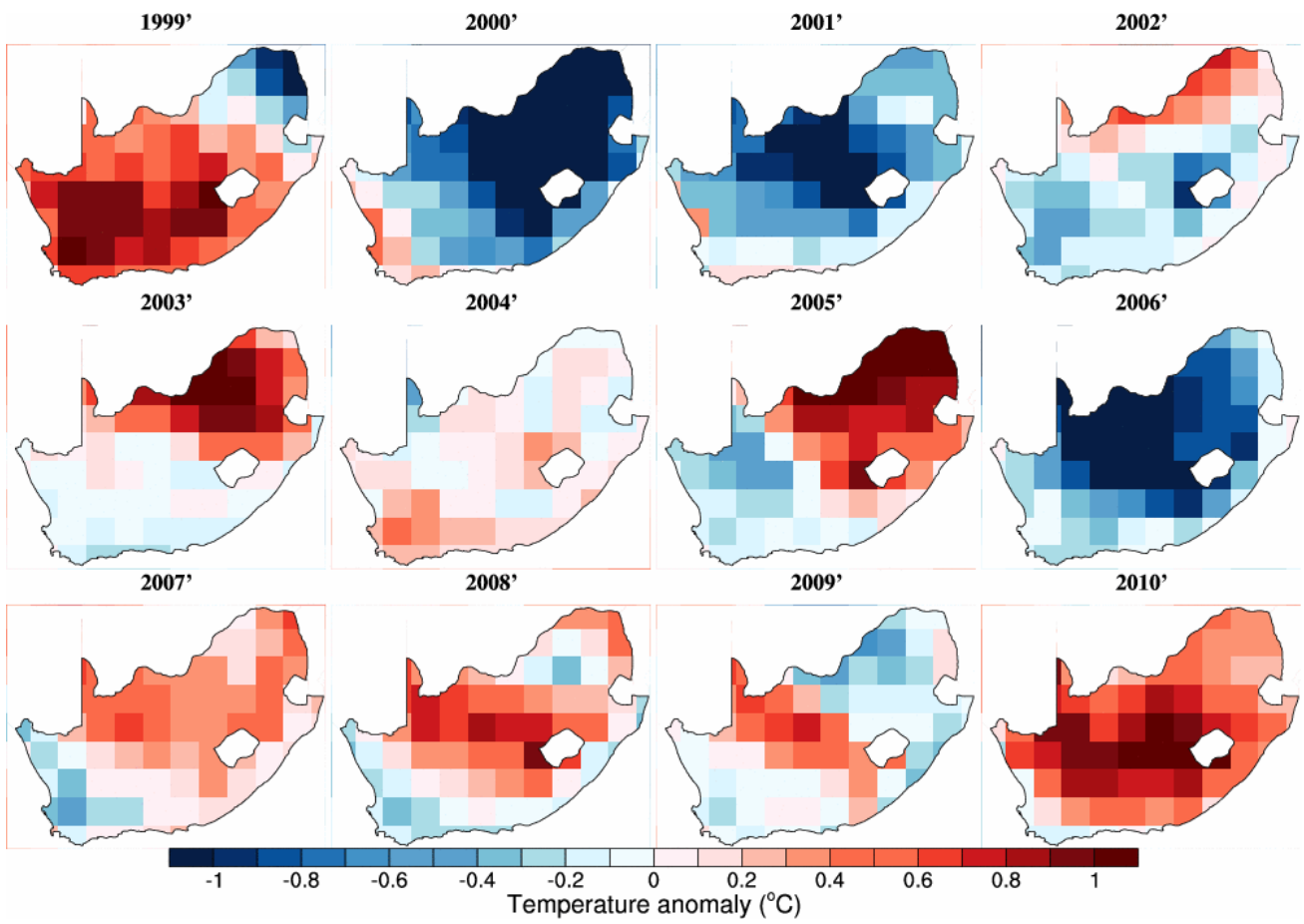


Fig SA6b: Annual temperature anomalies over South Africa (ERAINTERIM, reference climatology: 1998-2010).

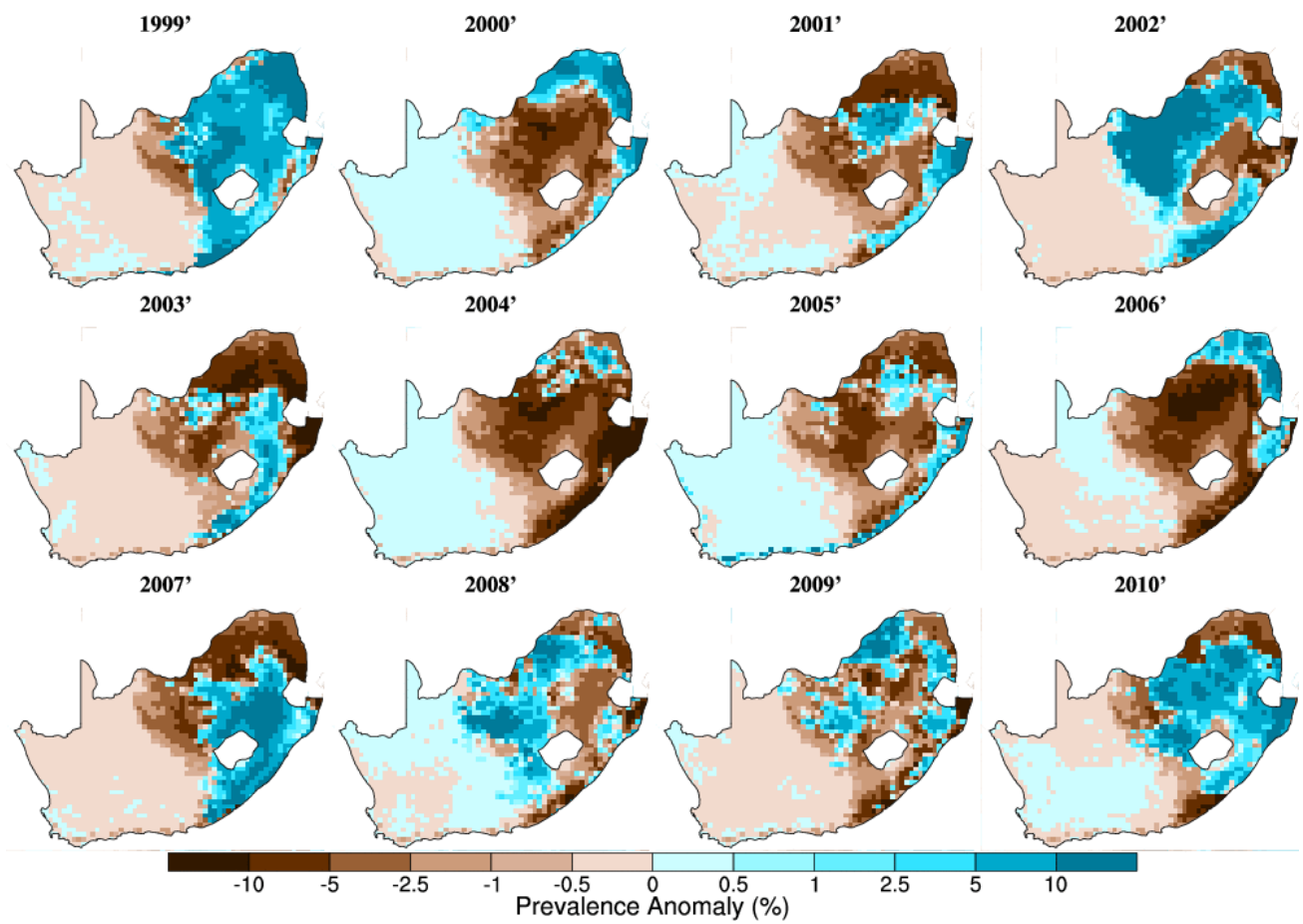


Fig SA6c: Annual malaria prevalence anomalies over South Africa (TRMM-ERA-Interim, reference climatology: 1998-2010).